Available online at http://scik.org
Commun. Math. Biol. Neurosci. 2025, 2025:84
https://doi.org/10.28919/cmbn/9305
ISSN: 2052-2541

EFFECT OF WIND AND DISEASE ON THE DYNAMICAL BEHAVIOR OF A PREY-PREDATOR SYSTEM

RASHA A. ALI[1,2], HIBA ABDULLAH IBRAHIM[1,*]

[1]Department of Mathematics, College of Science, University of Baghdad, Baghdad, Iraq

[2]Theoretical Sciences Department, College of Physical Education and Sports Science, University of Baghdad, Baghdad, Iraq

Abstract: Considering the significance of prey-predator models in the environment, these models illustrate the relationship between living things and their interactions. In this paper, a prey-predator model was advanced and studied that included the wind flow and disease in prey. This study aims to understand how these factors affect the behavior of species. The solution properties of the proposed model were examined. Also, all potential equilibrium points and their stability were studied. In addition, the persistence conditions that ensure the continued existence of organisms were calculated. The theoretical results were supported by numerical analysis by using the MATLAB program (version R2018b), which also explained how changing parameter values affected the dynamic behavior of the prey-predator model. Our findings suggest that diseases in prey have different effects on the proposed system, which can both stabilize or destabilize it. On the other hand, the wind flow represents a significant abiotic factor in the environment that affects the predation process. It is found that increasing the wind flow causes the extinction of the predator, which means the effect of wind flow acts as a bar to the search for food and decreases the efficiency of predators.

Keywords: equilibrium points; local bifurcation; persistence; prey-predator; stability analysis; wind flow.

2020 AMS Subject Classification: 92D25.

---

[*]Corresponding author
E-mail address: hiba.ibrahim@sc.uobaghdad.edu.iq
Received April 20, 2025

1. INTRODUCTION

Due to the large spread and significance of the interaction between predators and their prey, it will continue to be a critical topic, see [1-9]. The Lotka-Volterra model between predator and their prey has been the subject of many good articles since it was introduced by Lotka and Volterra [10,11]. Many modifications have been made to the basic model of the Lotka-Volterra model [12-16]. In the last decades, many mathematical biologists have tried to merge the ecology and epidemiology areas. The term Eco-epidemiological indicates to the incorporation of infection disease into the ecosystems [17]. It is well known that species in nature do not live alone. Really, any habitat may include dozens, hundreds or sometimes thousands of species. So, the possibility of disease spreading in the community becomes greater as the infected species increases. Therefore, studying the impact of disease on the dynamic behavior of interacting species is a vital biological importance in the environment [18-27].

Various mathematical models have been developed to analyze these effects, revealing complex relationships between disease spread in prey and predator responses. When analyzing the impacts of disease on the environment, disease in a prey [28-31], disease in a predator [32-35] and disease in both of them [36-39] can all be taken into account. All of these models illustrated that infection disease could cause fundamental changes in ecosystem dynamics. Predators may be eating susceptible and infected animals if the disease is existing in the prey. The interaction between predator and their prey can be affected by a set of factors. In these models, many researchers have been taken different environmental factors that can affect the presence and stability of the models as fear in prey populations [40- 42], anti-predator [43-45], hunting cooperation [46-48], stage structure [49-50] and many other factors that affect the dynamics of the system.

Ibrahim and Naji [51] suggested the effect of fear and harvesting in a prey-predator model with disease in a prey. They found that the disease and harvesting cause the extinction of one or more species, while the effect of fear leads to the stabilization of the system.

An ecological system contains biotic (living organisms) and abiotic (physical environment) factors that work together as a single unit. Different studies have been focused on biotic factors (the influences of any living components on the other organisms), while abiotic factors (the influences of nonliving components of the environment on living organisms) in ecological system have been less studied. In the last decades, many valuable studies have been behaved that consider the effect of temperature, water and wind flow differences on ecological systems [52].

The wind flow plays a critical role in the interactions between prey and predator with effects that can strengthen or dampen the impact of predators on their prey, for instance, [53-55]. Barman et al. [53] formulated and studied a prey–predator model involving wind flow in the predation function. They found complex dynamics under wind flow states. Also, Takyi et al. [54] introduced the dynamics of a prey-predator model that contains wind flow and prey refuge. Their results referred that the wind flow has both stabilizing and destabilizing influences on the system, while the prey refuge can stabilize the system and also increase the density of the prey and decrease the density of the predators.

On the other hand, Panja [55] suggested a prey-predator model with wind flow and anti-predator behavior. He found the effect of anti-predator behavior and wind flow can stabilize the system.

To the best of our understanding, very few studies have been conducted on examining the wind effects on predator-prey dynamics in a mathematical eco-epidemiological model. This inspires the effort to present this research paper. Recently,

This paper analyzes the impact of disease on prey population, specifically focusing on a susceptible-infected (SI) model. It highlights the wind flow affecting population interactions and stability. This article is structured as follows: Section 2 is formulated an eco-epidemiological model under the influence of wind flow. Section 3 is showed that the properties of the solution of the proposed model. While section 4 is appeared the existence of all feasible equilibrium points. Section 5 is discussed local stability at various equilibrium points. Section 6 Persistence of the model is discussed. Section 7 is offered the global stability of feasible equilibrium points. Further, section 8 with the help of the bifurcation theory, the local bifurcation is examined. Numerical analyses are conducted to numerically verify our analytical results in Section 9. Section 10 is contained conclusion and discussion.

2. MATHEMATICAL MODEL EQUATIONS

In this section, a prey-predator model involving infectious disease in prey under wind flow factor is formulate and study. The disease spreads by contact between susceptible and infected prey. The suggested model includes a modified Holling type II functional response in a windy environment as suggested in [56]. The following assumptions adopt to formulate the model.

1. Prey populations are divided into two categories: susceptible and infected individuals, where the susceptible and infected prey densities at time t denote by $S(t)$ and $I(t)$, respectively. While the predator density at time t denotes by $Z(t)$.

2. The prey grows logistically in the absence of predator with an intrinsic growth rate $(r > 0)$ and carrying capacity $(k > 0)$. It is supposed that the infected prey cannot reproduce or grow, due to the disease makes it weak. Furthermore, they still compete with susceptible for space and food.
3. The susceptible prey population becomes infected by contact with an infection rate $(\mu > 0)$, the infected prey does not recover from the disease is assumed.
4. The infected prey, weak and more vulnerable, is available for predators to predate, but this does not prevent the susceptible prey from being attacked by predators. Also the hindrance rate in susceptible and infected prey catching for the predator denoted by $(\beta_1, \beta_2 > 0)$.
5. The predator consumes both the susceptible and infected prey according to modified Holling type-II functional response containing the wind flow in the predation function with maximum attack rates $(\gamma_1, \gamma_2 > 0)$ whereas $(e_1, e_2 > 0)$ are indicate the conversion rates of predator, where $0 < e_i < 1$, for $i = 1,2$.
6. The natural mortality rate of predators is indicated by θ_1 while θ_2 the mortality rate of the infected prey encompasses both natural and disease-related mortality rates.
7. In a windy environment, increased wind flow reduces the predator's search efficiency. Let $\pi(\omega) = \frac{1}{1+\omega}$ be the wind efficiency under the following assumptions:
   i. In the absence of wind flow, the predator's search efficiency remains the same as before, i.e. $\pi(0) = 1$.
   ii. As wind flow increases, the predator search efficiency decreases continuously, i.e. $\pi'(\omega) < 0$.
   iii. Due to the large amount of wind flow, the predator cannot view any prey for its food resources, i.e. $\lim_{\omega \to \infty} \pi(\omega) = 0$.

From the above assumptions, the mathematical model is formulating as follow

$$\begin{aligned} \frac{dS}{dt} &= rS\left(1 - \frac{S+I}{K}\right) - \mu SI - \frac{\gamma_1 SZ}{1+\omega+\beta_1 S+\beta_2 I}, \\ \frac{dI}{dt} &= \mu SI - \frac{\gamma_2 IZ}{1+\omega+\beta_1 S+\beta_2 I} - \theta_1 I, \\ \frac{dZ}{dt} &= \frac{e_1\gamma_1 SZ + e_2\gamma_2 IZ}{1+\omega+\beta_1 S+\beta_2 I} - \theta_2 Z, \end{aligned} \tag{1}$$

with initial conditions, $S(0) = S_0 \geq 0, I(0) = I_0 \geq 0, Z(0) = Z_0 \geq 0$.

In the right hand side of the system (1), the interaction functions are continuous and have continuous partial derivatives on R_+^3. Therefore, the functions in system (1) are Lipschitizian functions. So system (1) has a unique solution. Moreover, in the following theorems, the positivity and bounded-ness of the solutions of system (1) are established.

3. Positivity and Bounded-Ness

To verify the well-posed of system (1), it suffices to prove all positive solutions remain positive for $0 \leq t < \infty$. From a biological point of view, positivity and bounded-ness confirm that the species interaction in our proposed system behaves ecologically well.

Theorem 3.1. All solution of system (1) with initial conditions exist starting in R_+^3, remain positive for all $t > 0$.

Proof.

Now, to investigate the positivity of system (1), integrate its equations and use the following positive initial conditions (S_0, I_0, Z_0) to get the following expressions:

From the system (1), it obtained

$$S(t) = S_0\, exp\left[\int_0^t \left\{r\left(1 - \frac{S(x)+I(x)}{k}\right) - \mu I(x) - \frac{\gamma_1 Z(x)}{1+\omega+\beta_1 S(x)+\beta_2 I(x)}\right\} dx\right] > 0,$$

Similarly,

$$I(t) = I_0\, exp\left[\int_0^t \left\{\mu S(x) - \frac{\gamma_2 Z(x)}{1+\omega+\beta_1 S(x)+\beta_2 I(x)} - \theta_1\right\} dx\right] > 0,$$

and

$$Z(t) = Z_0\, exp\left[\int_0^t \left\{\frac{e_1\gamma_1 S(x)+e_2\gamma_2 I(x)}{1+\omega+\beta_1 S(x)+\beta_2 I(x)} - \theta_2\right\} dx\right] > 0.$$

Given the above equations and the definition of an exponential function, any solution starting with positive initial conditions (S_0, I_0, Z_0) remains positive. Hence, the proof of the theorem is completed. ■

Theorem 3.2. In system (1), All solutions beginning in R_+^3 are uniformly bounded.

Proof. From system (1), the first equation can be written as

$$\frac{dS(t)}{dt} \leq rS\left(1 - \frac{S}{k}\right)$$

Hence, by solving the above differential inequality, it is obtained that

$$\lim_{t\to\infty} \sup S(t) \leq k.$$

A solution of system (1) can be represented as follows $B(t) = S(t) + I(t) + Z(t)$. After that, by using the derivative about t, it is obtained that

$$\frac{dB}{dt} = rS\left(1 - \frac{S+I}{k}\right) - \mu SI - \frac{\gamma_1 SZ}{1+\omega+\beta_1 S+\beta_2 I} + \mu SI - \frac{\gamma_2 IZ}{1+\omega+\beta_1 S+\beta_2 I}$$
$$-\theta_1 I + \frac{e_1\gamma_1 SZ + e_2\gamma_2 IZ}{1+\omega+\beta_1 S+\beta_2 I} - \theta_2 Z.$$

So, $\frac{dB}{dt} \leq k(1+r) - \xi B$, where $\xi = min\{1, \theta_1, \theta_2\}$ and this gives that $\frac{dB}{dt} + \xi B \leq k(1+r)$. Hence, due to the Grönwall Differential Inequality and for $t \to \infty$, it is obtained, $B(t) \leq \frac{k(1+r)}{\xi}$. Hence, all solutions of the system that begin in R_+^3 remain confined to the region Λ for all time.

$$\Lambda = \left\{(S, I, Z): 0 < S(t) \leq k; 0 \leq B(t) \leq \frac{k(1+r)}{\xi}, \xi = min\{1, \theta_1, \theta_2\}\right\}. \blacksquare$$

4. Existence of Equilibrium Points

In this section, the presence of all equilibrium points (biologically feasible) of the system (1) are discussed. It is noted that system (1) contains five equilibrium points at most, which can be determined as follows:

i. The population vanishing equilibrium point (PVEP) represented by $E_0 = (0,0,0)$ always existence.

ii. The Axial equilibrium point (AEP) represented by $E_1 = (k, 0,0)$ always existence.

iii. The predator-free equilibrium point (PF-EP) represented by $E_2 = (\bar{S}, \bar{I}, 0)$, where $\bar{S} = \frac{\theta_1}{\mu}$ and $\bar{I} = \frac{r(k-\bar{S})}{k\mu+r}$. Note that, the E_2 exists under the following condition is met.

$$\bar{S} < k \tag{2}$$

iv. The infected prey-free equilibrium point (IPF-EP) is denoted by $E_3 = (\hat{S}, 0, \hat{Z})$, where $\hat{S} = \frac{\theta_2(1+\omega)}{e_1\gamma_1 - \theta_2\beta_1}$ and $\hat{Z} = \frac{r(k-\hat{S})(1+\omega+\beta_1\hat{S})}{k\Upsilon_1}$. Moreover, the E_3 exists under the following condition is met.

$$\beta_1\theta_2 < e_1\Upsilon_1 \tag{3}$$
$$\hat{S} < k \tag{4}$$

v. The interior equilibrium point (I-EP) denoted by $E_4 = (S^*, I^*, Z^*)$, where

$$S^* = \frac{\theta_2\gamma_2(1+\omega)(r+k\mu) - k(e_2\gamma_2 - \theta_2\beta_2)(r\gamma_2 + \gamma_1\theta_1)}{\gamma_2(r+k\mu)(e_1\gamma_1 - \theta_2\beta_1) - (e_2\gamma_2 - \theta_2\beta_2)(r\gamma_2 + k\gamma_1\mu)}, I^* = \frac{\theta_2(1+\omega) - (e_1\gamma_1 - \theta_2\beta_1)S^*}{(e_2\gamma_2 - \theta_2\beta_2)},$$

and $Z^* = \frac{(\mu S^* - \theta_1)(1+\omega+\beta_1 S^* + \beta_2 I^*)}{\gamma_2}$. Therefore, when the condition (3) holds, E_4 exists if one of the following sets of additional conditions are met.

$$\left.\begin{matrix} e_2\gamma_2 < \theta_2\beta_2 \\ Max\{\hat{S},\bar{S}\} < S^* \end{matrix}\right\} \tag{5}$$

$$\left.\begin{matrix} \theta_2\beta_2 < e_2\gamma_2 \\ \bar{S} < S^* < \hat{S} \end{matrix}\right\} \tag{6}$$

5. LOCAL STABILITY ANALYSIS

In this section, the local stability of the system (1) around each equilibrium point is analyzed by finding the eigenvalues of the related Jacobian matrices. As stated in this, an equilibrium point is locally asymptotically stable (LAS) if the Jacobian matrix of the related equilibrium point has all eigenvalues with negative real parts and unstable if at least one or all eigenvalues becomes positive. The Jacobian matrix $J(S,I,Z)$ can be expressed as

$$J(S,I,Z) = \begin{bmatrix} \tau_{11} & \tau_{12} & \tau_{13} \\ \tau_{21} & \tau_{22} & \tau_{23} \\ \tau_{31} & \tau_{32} & \tau_{33} \end{bmatrix}, \tag{7}$$

where

$$\tau_{11} = r\left(1-\frac{2S+I}{k}\right) - \frac{\gamma_1 Z(1+\omega+\beta_2 I)}{(1+\omega+\beta_1 S+\beta_2 I)^2} - \mu I,\ \tau_{12} = S\left(\frac{-r}{k} - \mu + \frac{\gamma_1\beta_2 Z}{(1+\omega+\beta_1 S+\beta_2 I)^2}\right),$$

$$\tau_{13} = \frac{-\gamma_1 S}{(1+\omega+\beta_1 S+\beta_2 I)},\ \tau_{21} = \mu I + \frac{\gamma_2\beta_1\, IZ}{(1+\omega+\beta_1 S+\beta_2 I)^2},\ \tau_{22} = \mu S - \frac{\gamma_2 Z(1+\omega+\beta_1 S)}{(1+\omega+\beta_1 S+\beta_1 I)^2} - \theta_1,$$

$$\tau_{23} = \frac{-\gamma_2 I}{(1+\omega+\beta_1 S+\beta_2 I)},\ \tau_{31} = \frac{e_1\gamma_1(1+\omega+\beta_2 I)Z - e_2\gamma_2\beta_1 IZ}{(1+\omega+\beta_1 S+\beta_2 I)^2},\ \tau_{32} = \frac{e_2\gamma_2(1+\omega+\beta_1 S)Z - e_1\gamma_1\beta_1 SZ}{(1+\omega+\beta_1 S+\beta_2 I)^2},$$

$$\tau_{33} = \frac{e_1\gamma_1 S + e_2\gamma_2 I}{1+\omega+\beta_1 S+\beta_2 I} - \theta_2.$$

5.1. THE LOCAL STABILITY ANALYSIS AT $\boldsymbol{E_0 = (0,0,0)}$

The Jacobian matrix of system (1) at E_0 can be written as,

$$J(E_0) = \begin{bmatrix} r & 0 & 0 \\ 0 & -\theta_1 & 0 \\ 0 & 0 & -\theta_2 \end{bmatrix} \tag{8}$$

Then the eigenvalues of $J(E_0)$ are $\lambda_{01} = r > 0$, $\lambda_{02} = -\theta_1 < 0$ and $\lambda_{03} = -\theta_2 < 0$. Thus, the equilibrium point E_0 is a saddle point.

5.2. THE LOCAL STABILITY ANALYSIS AT $\boldsymbol{E_1 = (k,0,0)}$

The Jacobian matrix of system (1) at E_1 can be written as:

$$J(E_1) = \begin{bmatrix} -r & -k\left(\frac{r}{k}+\mu\right) & \frac{-k\gamma_1}{1+\omega+k\beta_1} \\ 0 & \mu k - \theta_1 & 0 \\ 0 & 0 & \frac{ke_1\gamma_1}{1+\omega+k\beta_1} - \theta_2 \end{bmatrix} \tag{9}$$

Then the eigenvalues of $J(E_1)$ are $\lambda_{11} = -r < 0$, $\lambda_{12} = \mu k - \theta_1$ and $\lambda_{13} = \frac{ke_1\gamma_1}{1+\omega+k\beta_1} - \theta_2$.

Thus, the equilibrium point E_1 is a LAS provided the following conditions are satisfied.

$$k < \bar{S} \tag{10}$$

$$\frac{ke_1\gamma_1}{1+\omega+k\beta_1} < \theta_2 \tag{11}$$

Furthermore, it is easy to prove that point E_1 is a saddle point if condition (2) is satisfied.

5.3. THE LOCAL STABILITY ANALYSIS AT $\boldsymbol{E_2 = (\bar{S}, \bar{I}, 0)}$

The Jacobian matrix of system (1) at E_2 can be written as:

$$J(E_2) = \begin{bmatrix} -\frac{r}{k}\bar{S} & \left(\frac{-r}{k} - \mu\right)\bar{S} & \frac{-\gamma_1\bar{S}}{(1+\omega+\beta_1\bar{S}+\beta_2\bar{I})} \\ \mu\bar{I} & 0 & \frac{-\gamma_2\bar{I}}{(1+\omega+\beta_1\bar{S}+\beta_2\bar{I})} \\ 0 & 0 & \frac{e_1\gamma_1\bar{S}+e_2\gamma_2\bar{I}}{(1+\omega+\beta_1\bar{S}+\beta_2\bar{I})} - \theta_2 \end{bmatrix} = [b_{ij}] \tag{12}$$

For all $i, j = 1,2,3$.

Obviously, the characteristic equation of $J(E_2)$ is

$$(\lambda^2 - (Trace_1)\lambda + Det_1)(b_{33} - \lambda) = 0. \tag{13}$$

here,

$$Trace_1 = -\frac{r}{k}\bar{S} < 0, \quad Det_1 = \mu\left(\frac{r}{k} + \mu\right)\bar{S}\bar{I} > 0.$$

Applying the Routh-Hawirtiz-criterion[44], all the eigenvalues of equation (13) have negative real parts and E_2 is a LAS if the following condition is met.

$$\frac{e_1\gamma_1\bar{S}+e_2\gamma_2\bar{I}}{(1+\omega+\beta_1\bar{S}+\beta_2\bar{I})} < \theta_2 \tag{14}$$

Moreover, E_2 is a saddle point with a stable manifold SI −plane when the condition (14) is reflected as the eigenvalue in the Z −direction becomes positive.

5.4. THE LOCAL STABILITY ANALYSIS AT $\boldsymbol{E_3 = (\hat{S}, 0, \hat{Z})}$

The Jacobian matrix of system (1) at E_3 can be written as:

$$J(E_3) = \begin{bmatrix} \frac{-r\hat{S}}{k} + \frac{\gamma_1\beta_1\hat{S}\hat{Z}}{(1+\omega+\beta_1\hat{S})^2} & \frac{\gamma_1\beta_2\hat{S}\hat{Z}}{(1+\omega+\beta_1\hat{S})^2} - \frac{r}{k}\hat{S} - \mu\hat{S} & \frac{-\gamma_1\hat{S}}{1+\omega+\beta_1\hat{S}} \\ 0 & \mu\hat{S} - \frac{\gamma_2\hat{Z}}{1+\omega+\beta_1\hat{S}} - \theta_1 & 0 \\ \frac{e_1\gamma_1(1+\omega)\hat{Z}}{(1+\omega+\beta_1\hat{S})^2} & \frac{e_2\gamma_2\hat{Z}(1+\omega+\beta_1\hat{S}) - e_1\gamma_1\beta_2\hat{S}\hat{Z}}{(1+\omega+\beta_1\hat{S})^2} & 0 \end{bmatrix} = [C_{ij}] \tag{15}$$

For all $i, j = 1,2,3$.

Obviously, the characteristic equation of $J(E_3)$ is

$$(\lambda^2 - (Trace_2)\lambda + Det_2)(C_{22} - \lambda) = 0. \tag{16}$$

here,

$$Trace_2 = -\frac{r\hat{S}}{k} + \frac{\gamma_1\beta_1\hat{S}\hat{Z}}{(1+\omega+\beta_1\hat{S})^2}, \quad Det_2 = \frac{e_1\gamma_1^2(1+\omega)\hat{S}\hat{Z}}{(1+\omega+\beta_1\hat{S})^3} > 0.$$

Applying the Routh-Hawirtiz-criterion[44], all the eigenvalues of equation (16) have negative real parts and E_3 is a LAS if the following conditions are met.

$$\mu\hat{S} < \frac{\gamma_2\hat{Z}}{1+\omega+\beta_1\hat{S}} + \theta_1 \tag{17}$$

$$\frac{\gamma_1\beta_1\hat{Z}}{(1+\omega+\beta_1\hat{S})^2} < \frac{r}{k} \tag{18}$$

Moreover, E_2 is a saddle point with a stable manifold SZ −plane when the condition (17) is reflected as the eigenvalue in the I −direction becomes a positive. However, it is a saddle with a stable manifold in the I −direction when condition (18) is reflected as the eigenvalues in the S −direction and that of Z −direction become positive. ■

5.5. THE LOCAL STABILITY ANALYSIS AT $E_4 = (S^*, I^*, Z^*)$

The Jacobian matrix of system (1) at E_4 can be written as:

$$J(E_4) = \begin{bmatrix} a_{11} & a_{12} & a_{13} \\ a_{21} & a_{22} & a_{23} \\ a_{31} & a_{32} & 0 \end{bmatrix} \tag{19}$$

here,

$$a_{11} = \left(-\frac{r}{k} + \frac{\gamma_1\beta_1 Z^*}{(1+\omega+\beta_1 S^*+\beta_2 I^*)^2}\right)S^*, \ a_{12} = \left(\frac{\gamma_1\beta_2 Z^*}{(1+\omega+\beta_1 S^*+\beta_2 I^*)^2} - \frac{r}{k} - \mu\right)S^*,$$

$$a_{13} = \frac{-\gamma_1 S^*}{1+\omega+\beta_1 S^*+\beta_2 I^*}, \ a_{21} = \left(\mu + \frac{\gamma_2\beta_1 Z^*}{(1+\omega+\beta_1 S^*+\beta_2 I^*)^2}\right)I^*, \ a_{22} = \frac{\gamma_2\beta_2 I^* Z^*}{(1+\omega+\beta_1 S^*+\beta_2 I^*)^2},$$

$$a_{23} = \frac{-\gamma_2 I^*}{1+\omega+\beta_1 S^*+\beta_2 I^*}, \ a_{31} = \frac{e_1\gamma_1 Z^*(1+\omega+\beta_2 I^*) - e_2\gamma_2\beta_1 I^* Z^*}{(1+\omega+\beta_1 S^*+\beta_2 I^*)^2},$$

$$a_{32} = \frac{e_2\gamma_2 Z^*(1+\omega+\beta_1 S^*) - e_1\gamma_1\beta_2 S^* Z^*}{(1+\omega+\beta_1 S^*+\beta_2 I^*)^2}, \ a_{33} = 0.$$

The characteristic equation for $E_4 = (S^*, I^*, Z^*)$ is as follows:

$$\lambda^3 + A_1^*\lambda^2 + A_2^*\lambda + A_3^* = 0, \tag{20}$$

where:

$$A_1^* = -(a_{11} + a_{22}),$$
$$A_2^* = (a_{11}a_{22} - a_{12}a_{21} - a_{13}a_{31} - a_{23}a_{32}),$$
$$A_3^* = a_{23}(a_{11}a_{32} - a_{12}a_{31}) + a_{13}(a_{22}a_{31} - a_{21}a_{32}).$$

So, by Routh–Hurwitz criterion, equation (21) has negative real parts provided that $A_1^* > 0$, $A_3^* > 0$, and $\Delta > 0$, where:

$$\Delta = A_1^* A_2^* - A_3^* = -(a_{11}+a_{22})(a_{11}a_{22}-a_{12}a_{21}) + a_{31}(a_{11}a_{13}+a_{12}a_{23}) + a_{32}(a_{22}a_{23}+a_{13}a_{21}).$$

Therefore, E_4 is a LAS, if the following conditions hold

$$\frac{Z^*(\gamma_1\beta_1 S^* + \gamma_2\beta_2 I^*)}{(1+\omega+\beta_1 S^* + \beta_2 I^*)^2} < \frac{rS^*}{k} \tag{21}$$

$$a_{11}a_{32} - a_{12}a_{31} < 0 \tag{22}$$

$$a_{22}a_{31} - a_{21}a_{32} < 0 \tag{23}$$

$$a_{11}a_{22} - a_{12}a_{21} > 0 \tag{24}$$

$$M_1 + M_2 > 0 \tag{25}$$

here,

$$M_1 = -(a_{11}+a_{22})(a_{11}a_{22}-a_{12}a_{21}) + a_{31}(a_{11}a_{13}+a_{12}a_{23}) > 0,$$
$$M_2 = a_{32}(a_{22}a_{23}+a_{13}a_{21}) < 0.$$

6. PERSISTENCE OF SYSTEM (1)

In this section, the persistence of system (1) is investigated. It is well recognized that system (1) is said to persist if and only if none of its species becomes extinct, this means system (1) will be persist if the system's trajectory that begins at a positive initial point doesn't has omega limit set on the boundary planes of the positive cone.

System (1) contains two sub-systems located in the $SI-$ and $SZ-$ planes, respectively, which can be described as follows:

$$\begin{aligned} \frac{dS}{dt} &= S\left(r\left(1-\frac{S+I}{K}\right) - \mu I\right) = g_1(S,I), \\ \frac{dI}{dt} &= I(\mu S - \theta_1) = g_2(S,I) \end{aligned} \tag{26}$$

and

$$\begin{aligned} \frac{dS}{dt} &= S\left(r\left(1-\frac{S}{K}\right) - \frac{\Upsilon_1 Z}{1+\omega+\beta_1 S}\right) = G_1(S,Z), \\ \frac{dZ}{dt} &= Z\left(\frac{e_1\Upsilon_1 S}{1+\omega+\beta_1 S} - \theta_2\right) = G_2(S,Z) \end{aligned} \tag{27}$$

It can be simply asserted that the above sub-systems (27) and (28) have positive equilibrium points that corresponding to those in system (1) in the interior of boundary planes $SI-$ and $SZ-$planes, respectively. Now, to explore the possibility of the presence of periodic oscillation in the boundary planes, the Dulac function is utilized.

Now, define the Dulac function as $H_1(S,I) = \frac{1}{SI}$. It's clear that, $H_1(S,I) > 0$ and C^1 function in the $Int.R_+^2$ of SI −plane. Furthermore, it is obtained that

$$\Delta(S,I)=\frac{\partial(H_1\, g_1)}{\partial S}+\frac{\partial(H_1\, g_2)}{\partial I}=-\frac{r}{kI} \tag{28}$$

Therefore, $\Delta(S,I)$ doesn't identically zero and doesn't alter sign. Therefore, there are no periodic oscillation in the interior positive quadrant of SI −plane for sub-system (26).

Similarly, by utilizing another Dulac function $H_2(S,Z)=\frac{1}{SZ}$. It's note that, $H_2(S,Z)>0$ and C^1 function in the $Int.\mathbb{R}_+^2$ of SZ −plane. Moreover, it is obtained that

$$\Delta(S,Z)=\frac{\partial(H_2\, G_1)}{\partial S}+\frac{\partial(H_2\, G_2)}{\partial Z}=-\frac{r}{kZ}+\frac{\gamma_1\,\beta_1}{(1+\omega+\beta_1 S)^2} \tag{29}$$

Clear that, no periodic oscillation is observed in the interior positive quadrant of the $SZ-$ plane of sub-system (27) under the following conditions:

$$\frac{\gamma_1\,\beta_1}{(1+\omega+\beta_1 S)^2}<\frac{r}{kZ} \tag{30}$$

or

$$\frac{r}{kZ}<\frac{\gamma_1\,\beta_1}{(1+\omega+\beta_1 S)^2} \tag{31}$$

Theorem 6.1. Assume that the boundary planes have no periodic oscillation if condition (30) or (31) are met. then system (1) is uniformly persistent as long as that condition (2) and the following conditions are met.

$$\theta_2<\frac{e_1\gamma_1 k}{1+\omega+\beta_1 k} \tag{32}$$

$$\theta_2<\frac{e_1\gamma_1\bar{S}+e_2\gamma_2\bar{I}}{1+\omega+\beta_1\bar{S}+\beta_2\bar{I}} \tag{33}$$

$$\frac{\gamma_2\hat{Z}}{1+\omega+\beta_1\hat{S}}+\theta_1<\mu\hat{S} \tag{34}$$

Proof. Consider an average Lyapunov function as $\zeta(S,I,Z)=S^{\zeta_1}I^{\zeta_2}Z^{\zeta_3};\forall\zeta_i;$ where ζ_i for $i=1,2,3$ are positive constants and $\zeta(S,I,Z)>0$ for all $(S,I,Z)\in Int.R_+^3$. with $\zeta(S,I,Z)\to 0$ $if\ S\to 0\ or\ I\to 0\ or\ Z\to 0$. Therefore, some calculation gives

$$\begin{aligned}\Omega(S,I,Z)=\frac{\dot{\zeta}\,(S,I,Z)}{\zeta(S,I,Z)}&=\zeta_1\left[r\left(1-\frac{S+I}{k}\right)-\mu I-\frac{\gamma_1 Z}{1+\omega+\beta_1 S+\beta_2 I}\right]\\ &+\zeta_2\left[\mu S-\frac{\gamma_2 Z}{1+\omega+\beta_1 S+\beta_2 I}-\theta_1\right]+\zeta_3\left[\frac{e_1\gamma_1 S+e_2\gamma_2 I}{1+\omega+\beta_1 S+\beta_2 I}-\theta_2\right].\end{aligned}$$

Now, by the average Lyapunov method, the proof is valid provided that $\Omega(S,I,Z)>0$ for all boundary equilibria of system (1). Therefore,

$$\Omega(E_0)=\zeta_1(r)+\zeta_2(-\theta_1)+\zeta_3(-\theta_2)$$

Clearly, by selecting the suitable positive value of ζ_1 sufficiently larger than that of $\zeta_2\ and\ \zeta_3$, it's got that $\Omega(E_0)>0$.

$$\Omega(E_1) = \zeta_2(\mu S - \theta_1) + \zeta_3\left(\frac{e_1\gamma_1 S}{1+\omega+\beta_1 S} - \theta_2\right).$$

Obviously, conditions (2) and (32) ensure that $\Omega(E_1) > 0$.

$$\Omega(E_2) = \zeta_3\left(\frac{e_1\gamma_1\bar{S}+e_2\gamma_2\bar{I}}{1+\omega+\beta_1\bar{S}+\beta_2\bar{I}} - \theta_2\right).$$

Visibly, condition (33) guarantees that $\Omega(E_2) > 0$.

$$\Omega(E_3) = \zeta_2\left(\mu\hat{S} - \frac{\gamma_2\hat{Z}}{1+\omega+\beta_1\hat{S}} - \theta_1\right).$$

Finally, condition (34) guarantees that $\Omega(E_3) > 0$. So, system (1) is uniformly persistent.

7. GLOBAL STABILITY ANALYSIS

In this section, the global stability of the equilibrium points of system (1) that are locally asymptotically stable LAS will be determined utilizing suitable Lyapunov functions.

Theorem 7.1. Presume that $E_1 = (k, 0,0)$ is LAS, then it's globally asymptotically stable if the following conditions are met

$$r + \mu k < \theta_1 \tag{35}$$

$$\frac{\gamma_1 k}{1+\omega} < \theta_2 \tag{36}$$

Proof. Consider a suitable Lyapunov function

$$\sigma_1(S, I, Z) = \int_{\check{S}}^{S} \frac{u_1 - \check{S}}{u_1} du_1 + I + Z.$$

Here, $\sigma_1(S, I, Z)$ is a positive definite function so that $\sigma_1(k, 0,0) = 0$, $\sigma_1(S, I, Z) > 0$ for all $(S, I, Z) \in R_+^3$ and $S > 0$. The time derivative of σ_1 is given by

$$\frac{d\sigma_1}{dt} = \left(S - \check{S}\right)\left[r\left(1 - \frac{S+I}{k}\right) - \mu I - \frac{\gamma_1 Z}{1+\omega+\beta_1 S+\beta_2 I}\right]$$
$$+\mu SI - \frac{\gamma_2 IZ}{1+\omega+\beta_1 S+\beta_2 I} - \theta_1 I$$
$$+\frac{e_1\gamma_1 SZ}{1+\omega+\beta_1 S+\beta_2 I} + \frac{e_2\gamma_2 IZ}{1+\omega+\beta_1 S+\beta_2 I} - \theta_2 Z$$

It was obtained through the use of basic algebraic calculations.

$$\frac{d\sigma_1}{dt} = \frac{-r}{k}(S - \check{S})^2 + \frac{r\check{S}I}{k} + \mu\check{S}I - \frac{(1-e_1)\gamma_1 SZ}{A} - \frac{(1-e_2)\gamma_2 IZ}{A} + \frac{\gamma_1\check{S}Z}{A} - \theta_1 I - \theta_2 Z,$$

where, $A = 1 + \omega + \beta_1 S + \beta_2 I$.

Hence, $\frac{d\sigma_1}{dt} \le -\frac{r}{k}(S-k)^2 - \left(\theta_1 - (r+\mu k)\right)I - \left(\theta_2 - \frac{\gamma_1 k}{1+\omega}\right)Z.$

Hence, utilizing conditions (35)-(36) lead to $\frac{d\sigma_1}{dt}$ is negative definite. Thus, E_1 is a globally asymptotically stable. □

Theorem 7.2. Presume that $E_2 = (\bar{S}, \bar{I}, 0)$ is LAS, then it's globally asymptotically stable if the following condition is met

$$\frac{\gamma_1 \bar{S} + \gamma_2 \bar{I}}{1+\omega} < \theta_2 \tag{37}$$

Proof. Consider a suitable Lyapunov function

$$\sigma_2(S, I, Z) = \int_{\bar{S}}^{S} \frac{u_1 - \bar{S}}{u_1} du_1 + \int_{\bar{I}}^{I} \frac{u_2 - \bar{I}}{u_2} du_2 + Z.$$

Here, $\sigma_2(S, I, Z)$ is a positive definite function so that $\sigma_2(\bar{S}, \bar{I}, 0) = 0$, $\sigma_2(S, I, Z) > 0$ for all $(S, I, Z) \in R_+^3$ and $S > 0$ and $I > 0$. The time derivative of σ_2 is given by

$$\frac{d\sigma_2}{dt} = (S - \bar{S}) \left[r\left(1 - \frac{S+I}{k}\right) - \mu I - \frac{\gamma_1 Z}{1 + \omega + \beta_1 S + \beta_2 I} \right]$$
$$+ (I - \bar{I}) \left[\mu S - \frac{\gamma_2 Z}{1 + \omega + \beta_1 S + \beta_2 I} - \theta_1 \right]$$
$$+ \frac{e_1 \gamma_1 S Z}{1 + \omega + \beta_1 S + \beta_2 I} + \frac{e_2 \gamma_2 I Z}{1 + \omega + \beta_1 S + \beta_2 I} - \theta_2 Z$$

It was obtained through the use of basic algebraic calculations.

$$\frac{d\sigma_2}{dt} = \frac{-r}{k}(S - \bar{S})^2 - \frac{r}{k}(S - \bar{S})(I - \bar{I}) - \mu(S - \bar{S})(I - \bar{I})$$
$$- \frac{\gamma_1 S Z}{A} + \frac{\gamma_1 \bar{S} Z}{A} + \mu(S - \bar{S})(I - \bar{I}) - \frac{\gamma_2 I Z}{A}$$
$$+ \frac{\gamma_2 \bar{I} Z}{A} + \frac{e_1 \gamma_1 S Z}{A} + \frac{e_2 \gamma_2 I Z}{A} - \theta_2 Z.$$

where, $A = 1 + \omega + \beta_1 S + \beta_2 I$.

$\frac{d\sigma_2}{dt} \leq \frac{-r}{k}(S - \bar{S})^2 - \frac{r}{k}(S - \bar{S})(I - \bar{I}) + \frac{(\gamma_1 \bar{S} + \gamma_2 \bar{I})Z}{A} - \theta_2 Z.$

Hence, $\frac{d\sigma_2}{dt} < \frac{-3r}{2k}(S - \bar{S})^2 - \frac{r}{2k}(I - \bar{I})^2 - Z\left[\theta_2 - \frac{\gamma_1 \bar{S} + \gamma_2 \bar{I}}{1+\omega}\right].$

Hence, utilizing condition (37) leads to $\frac{d\sigma_2}{dt}$ is negative definite. Thus, E_2 is a globally asymptotically stable. □

Theorem 7.3. Presume that $E_3 = \left(\hat{S}, 0, \hat{Z}\right)$ is LAS, then it's globally asymptotically stable fulfilled the following conditions are met

$$\left(\frac{r}{k} + \mu\right)\hat{S} + \frac{\gamma_1 \beta_2 k \hat{Z}}{(1+\omega)(1+\omega+\beta_1 \hat{S})} < \theta_1 + \frac{e_2 \gamma_2 \hat{Z}}{(1+\omega)} \tag{38}$$

$$\frac{\gamma_1 \beta_1 \hat{Z}}{(1+\omega+\beta_1 \hat{S})} < \frac{r(1+\omega)}{k} + \frac{\gamma_1(\beta_1 \hat{S} + (1+\omega)(1-e_1))}{2(1+\omega+\beta_1 \hat{S})} \tag{39}$$

Proof. Consider a suitable Lyapunov function

$$\sigma_3(S,I,Z) = \int_{\hat{S}}^{S} \frac{u_1 - \hat{S}}{u_1} du_1 + I + \int_{\hat{Z}}^{Z} \frac{u_3 - \hat{Z}}{u_3} du_3.$$

Here, $\sigma_3(S,I,Z)$ is a positive definite function so that $\sigma_3(\hat{S},0,\hat{Z}) = 0$, $\sigma_3(S,I,Z) > 0$ for all $(S,I,Z) \in R_+^3$ and $S > 0$ and $Z > 0$. The time derivative of σ_3 is given by

$$\frac{d\sigma_3}{dt} = (S-\hat{S})\left[r\left(1-\frac{S+I}{k}\right) - \mu I - \frac{\gamma_1 Z}{1+\omega+\beta_1 S+\beta_2 I}\right] + \mu SI - \frac{\gamma_2 IZ}{1+\omega+\beta_1 S+\beta_2 I} - \theta_1 I$$
$$+(Z-\hat{Z})\left[\frac{e_1\gamma_1 S}{1+\omega+\beta_1 S+\beta_2 I} + \frac{e_2\gamma_2 I}{1+\omega+\beta_1 S+\beta_2 I} - \theta_2\right].$$

It was obtained through the use of basic algebraic calculations.

$$\frac{d\sigma_3}{dt} = -\frac{r}{k}(S-\hat{S})^2 - \frac{r}{k}SI + \mu SI + \left(\frac{r}{k}+\mu\right)\hat{S}I - \frac{\gamma_1(1+\omega)}{A\hat{A}}(S-\hat{S})(Z-\hat{Z})$$
$$+\frac{\gamma_1\beta_2 SI\hat{Z}}{A\hat{A}} - \frac{\gamma_1\beta_2\hat{S}I\hat{Z}}{A\hat{A}} + \frac{\gamma_1\beta_1\hat{Z}}{A\hat{A}}(S-\hat{S})^2 - \frac{\gamma_1\beta_1\hat{S}}{A\hat{A}}(S-\hat{S})(Z-\hat{Z})$$
$$+\mu SI - \frac{\gamma_2 IZ}{A} - \theta_1 I + \frac{e_1\gamma_1(1+\omega)}{A\hat{A}}(S-\hat{S})(Z-\hat{Z})$$
$$-\frac{e_1\gamma_1\beta_2\hat{S}IZ}{A\hat{A}} + \frac{e_1\gamma_1\beta_2\hat{S}I\hat{Z}}{A\hat{A}} + \frac{e_2\gamma_2 IZ}{A} - \frac{e_2\gamma_2 I\hat{Z}}{A}.$$

Therefore,

$$\frac{d\sigma_3}{dt} \le -\left[\frac{r}{k} - \frac{\gamma_1\beta_1\hat{Z}}{A\hat{A}}\right](S-\hat{S})^2 + \left(\frac{r}{k}+\mu\right)\hat{S}I - \left[\frac{\gamma_1\left(\beta_1\hat{S}+(1+\omega)(1-e_1)\right)}{A\hat{A}}\right](S-\hat{S})(Z-\hat{Z})$$
$$+\frac{\gamma_1\beta_2 SI\hat{Z}}{A\hat{A}} - \theta_1 I - \frac{e_2\gamma_2 I\hat{Z}}{A}.$$

where, $A = 1+\omega+\beta_1 S+\beta_2 I$, and $\hat{A} = 1+\omega+\beta_1\hat{S}$.

Hence,

$$\frac{d\sigma_3}{dt} < -\left[\frac{r}{k} - \frac{\gamma_1(2\beta_1\hat{Z}+\beta_1\hat{S}+(1+\omega)(1-e_1))}{2A\hat{A}}\right](S-\hat{S})^2 - \left[\frac{\gamma_1(\beta_1\hat{S}+(1+\omega)(1-e_1))}{2A\hat{A}}\right](Z-\hat{Z})^2$$
$$-I\left[\theta_1 + \frac{e_2\gamma_2\hat{Z}}{A} - \left(\frac{r}{k}+\mu\right)\hat{S} - \frac{\gamma_1\beta_2 S\hat{Z}}{A\hat{A}}\right].$$

Hence, utilizing conditions (38)-(39) lead to $\frac{d\sigma_3}{dt}$ is negative definite. Thus, E_3 is a globally asymptotically stable. □

Theorem 7.4. Presume that $E_4 = (S^*,I^*,Z^*)$ is LAS, then it's globally asymptotically stable fulfilled the following condition is met

$$Z^* < min\left\{\frac{\gamma_1(1-e_1)(1+\omega+\beta_2 I^*)+\beta_1(\gamma_1 S^*+e_2\gamma_2 I^*)}{2\gamma_1\beta_1+\gamma_1\beta_2+\gamma_2\beta_1}, \frac{\gamma_2(1-e_2)(1+\omega+\beta_1 S^*)+\beta_2(\gamma_2 I^*+e_1\gamma_1 S^*)}{2\gamma_2\beta_2+\gamma_1\beta_2+\gamma_2\beta_1}\right\} \quad (40)$$

Proof. Consider a suitable Lyapunov function

$$\sigma_4(S,I,Z)=\int_{S^*}^{S}\frac{u_1-S^*}{u_1}du_1+\int_{I^*}^{I}\frac{u_2-I^*}{u_2}du_2+\int_{Z^*}^{Z}\frac{u_3-Z^*}{u_3}du_3.$$

Here, $\sigma_4(S,I,Z)$ is a positive definite function so that $\sigma_4(S^*,I^*,Z^*)=0$, $\sigma_4(S,I,Z)>0$ for all $(S,I,Z)\in R_+^3$ and $S>0$, $I>0$ and $Z>0$. The time derivative of σ_4 is given by

$$\frac{d\sigma_4}{dt}=(S-S^*)\left[r\left(1-\frac{S+I}{k}\right)-\mu I-\frac{\gamma_1 Z}{1+\omega+\beta_1 S+\beta_2 I}\right]+(I-I^*)\left[\mu S-\frac{\gamma_2 Z}{1+\omega+\beta_1 S+\beta_2 I}-\theta_1\right]$$
$$+(Z-Z^*)\left[\frac{e_1\gamma_1 S}{1+\omega+\beta_1 S+\beta_2 I}+\frac{e_2\gamma_2 I}{1+\omega+\beta_1 S+\beta_2 I}-\theta_2\right]$$

It was obtained through the use of basic algebraic calculations.

$$\frac{d\sigma_4}{dt}=-\left(\frac{r}{k}-\frac{\gamma_1\beta_1 Z^*}{AA^*}\right)(S-S^*)^2-\left(\frac{r}{k}-\frac{\gamma_1\beta_2 Z^*}{AA^*}-\frac{\gamma_2\beta_1 Z^*}{AA^*}\right)(S-S^*)(I-I^*)$$
$$-(\frac{-\gamma_2\beta_2 Z^*}{AA^*})(I-I)^2$$
$$-\left[\frac{\gamma_1(1+\omega)}{AA^*}+\frac{\gamma_1\beta_1 S^*}{AA^*}+\frac{\gamma_1\beta_2 I^*}{AA^*}-\frac{e_1\gamma_1(1+\omega)}{AA^*}-\frac{e_1\gamma_1\beta_2 I^*}{AA^*}+\frac{e_2\gamma_2\beta_1 I^*}{AA^*}\right](S-S^*)(Z-Z^*).$$
$$-\left[\frac{\gamma_2(1+\omega)}{AA^*}+\frac{\gamma_2\beta_1 S^*}{AA^*}+\frac{\gamma_2\beta_2 I^*}{AA^*}+\frac{e_1\gamma_1\beta_2 S^*}{AA^*}-\frac{e_2\gamma_2(1+\omega)}{AA^*}-\frac{e_2\gamma_2\beta_1 S^*}{AA^*}\right](I-I^*)(Z-Z^*)$$

Moreover

$$\frac{d\sigma_4}{dt}=-\left(\frac{r}{k}-\frac{\gamma_1\beta_1 Z^*}{AA^*}\right)(S-S^*)^2-\left(\frac{r}{k}-\frac{Z^*}{AA^*}(\gamma_1\beta_2+\gamma_2\beta_1)\right)(S-S^*)(I-I^*)$$
$$+\left(\frac{\gamma_2\beta_2 Z^*}{AA^*}\right)(I-I^*)^2$$
$$-\frac{1}{AA^*}[\gamma_1(1-e_1)(1+\omega+\beta_2 I^*)+\beta_1(\gamma_1 S^*+e_2\gamma_2 I^*)](S-S^*)(Z-Z^*).$$
$$-\frac{1}{AA^*}[\gamma_2(1-e_2)(1+\omega+\beta_1 S^*)+\beta_2(\gamma_2 I^*+e_1\gamma_1 S^*)](I-I^*)(Z-Z^*)$$

where, $A=1+\omega+\beta_1 S+\beta_2 I$, and $A^*=1+\omega+\beta_1 S^*+\beta_2 I^*$.

Hence,

$$\frac{d\sigma_4}{dt}<-\rho_1(S-S^*)^2-\rho_2(I-I^*)^2-\rho_3(Z-Z^*)^2$$

here,

$\rho_1=\frac{1}{2}\left[\frac{3r}{k}+\frac{\gamma_1(1-e_1)(1+\omega+\beta_2 I^*)+\beta_1(\gamma_1 S^*+e_2\gamma_2 I^*)}{AA^*}-\frac{Z^*}{AA^*}(2\gamma_1\beta_1+\gamma_1\beta_2+\gamma_2\beta_1)\right]$,

$\rho_2=\frac{1}{2}\left[\frac{r}{k}+\frac{\gamma_2(1-e_2)(1+\omega+\beta_1 S^*)+\beta_2(\gamma_2 I^*+e_1\gamma_1 S^*)}{AA^*}-\frac{2\gamma_2\beta_2 Z^*}{AA^*}-\frac{Z^*}{AA^*}(2\gamma_2\beta_2+\gamma_1\beta_2+\gamma_2\beta_1)\right]$, and

$\rho_{3=}\frac{1}{2AA^*}[\gamma_1(1-e_1)(1+\omega+\beta_2 I^*)+\gamma_2(1-e_2)(1+\omega+\beta_1 S^*)+\beta_1(\gamma_1 S^*+e_2\gamma_2 I^*)+$ $\beta_2(\gamma_2 I^*+e_1\gamma_1 S^*)]$.

Hence, utilizing condition (40) lead to $\frac{d\sigma_4}{dt}$ is negative definite. Thus, E_4 is a globally asymptotically stable. □

8. BIFURCATION ANALYSIS

In this section, Sotomayor's theorem [57] is utilized to identify the local bifurcation near the equilibrium points of system (1). It is known that the presence of a non-hyperbolic equilibrium point is a necessary but not sufficient condition for bifurcation to happen. Thus, the candidate bifurcation parameter is chosen such that the equilibrium point is non-hyperbolic at a particular value of that parameter.

Now, expressing system (1) in the following:

$\frac{d\boldsymbol{X}}{dt} = \boldsymbol{G}(\boldsymbol{X})$, where $\boldsymbol{X} = (S, I, Z)^T$, $\boldsymbol{G} = (Sg_1, Ig_2, Zg_3)^T$, with $g_i; i = 1,2,3$ represent the interaction functions in the right-hand side of system (1). Let $\boldsymbol{V} = (v_1, v_2, v_3)^T$ be any non-zero vector, then the direct calculations on the Jacobian matrix of system (1) give the second and third directional derivatives:

$$D^2\boldsymbol{G}(S,I,Z)(\boldsymbol{V},\boldsymbol{V}) = [c_{i1}]_{3\times 1}, i = 1,2,3 \tag{41}$$

$$\begin{aligned}
c_{11} = {} & 2\left[-\frac{r}{k} + \frac{\gamma_1\beta_1 Z(1+\omega+\beta_2 I)}{(1+\omega+\beta_1 S+\beta_2 I)^3}\right] v_1^2 + 2\left[-\left(\frac{r}{k}+\mu\right) + \frac{\gamma_1\beta_2 Z(1+\omega-\beta_1 S+\beta_2 I)}{(1+\omega+\beta_1 S+\beta_2 I)^3}\right] v_1 v_2 \\
& +2\left[-\frac{\gamma_1(1+\omega+\beta_2 I)}{(1+\omega+\beta_1 S+\beta_2 I)^2}\right] v_1 v_3 \\
& +2\left[-\frac{\gamma_1\beta_2^2 SZ}{(1+\omega+\beta_1 S+\beta_2 I)^3}\right] v_2^2 + 2\left[\frac{\gamma_1\beta_2 S}{(1+\omega+\beta_1 S+\beta_2 I)^2}\right] v_2 v_3
\end{aligned}$$

$$\begin{aligned}
c_{21} = {} & 2\left[-\frac{\gamma_2\beta_1^2 IZ}{(1+\omega+\beta_1 S+\beta_2 I)^3}\right] v_1^2 + 2\left[\mu + \frac{\gamma_2\beta_1 Z(1+\omega+\beta_1 S-\beta_2 I)}{(1+\omega+\beta_1 S+\beta_2 I)^3}\right] v_1 v_2 \\
& +2\left[\frac{\gamma_2\beta_1 I}{(1+\omega+\beta_1 S+\beta_2 I)^2}\right] v_1 v_3 \\
& +2\left[\frac{\gamma_2\beta_2 Z(1+\omega+\beta_1 S)}{(1+\omega+\beta_1 S+\beta_2 I)^3}\right] v_2^2 + 2\left[-\frac{\gamma_2(1+\omega+\beta_1 S)}{(1+\omega+\beta_1 S+\beta_2 I)^2}\right] v_2 v_3.
\end{aligned}$$

$$\begin{aligned}
c_{31} = {} & 2\left[\frac{\beta_1 Z(e_2\gamma_2\beta_1 I - (1+\omega+\beta_2 I)e_1\gamma_1)}{(1+\omega+\beta_1 S+\beta_2 I)^3}\right] v_1^2 + 2\left[\frac{-Z\big(e_1\gamma_1\beta_2(1+\omega-\beta_1 S+\beta_2 I)+e_2\gamma_2\beta_1(1+\omega+\beta_1 S-\beta_2 I)\big)}{(1+\omega+\beta_1 S+\beta_2 I)^3}\right] v_1 v_2 \\
& +2\left[\frac{(1+\omega+\beta_2 I)e_1\gamma_1 - e_2\gamma_2\beta_1 I}{(1+\omega+\beta_1 S+\beta_2 I)^2}\right] v_1 v_3 \\
& +2\left[\frac{\beta_2 Z(e_1\gamma_1\beta_2 S - (1+\omega+\beta_1 S)e_2\gamma_2}{(1+\omega+\beta_1 S+\beta_2 I)^3}\right] v_2^2 + 2\left[\frac{(1+\omega+\beta_1 S)e_2\gamma_2 - e_1\gamma_1\beta_2 S}{(1+\omega+\beta_1 S+\beta_2 I)^2}\right] v_2 v_3
\end{aligned}$$

While

$$D^3\boldsymbol{G}(S,I,Z)\,(\boldsymbol{V},\boldsymbol{V},\boldsymbol{V}) = [d_{i1}]_{3\times 1}, i = 1,2,3 \tag{42}$$

where

$$d_{11} = 6\left[-\frac{\gamma_1\beta_1^2 Z(1+\omega+\beta_2 I)}{(1+\omega+\beta_1 S+\beta_2 I)^4}\right] v_1^3 + 6\left[\frac{\gamma_1\beta_1\beta_2 Z(2(1+\omega+\beta_2 I)+\beta_1 S)}{(1+\omega+\beta_1 S+\beta_2 I)^4}\right] v_1^2 v_2 + 6\left[\frac{\gamma_1\beta_1(1+\omega+\beta_2 I)}{(1+\omega+\beta_1 S+\beta_2 I)^3}\right] v_1^2 v_3 + 6\left[-\frac{\gamma_1\beta_2^2 Z(1+\omega-2\beta_1 S+\beta_2 I)}{(1+\omega+\beta_1 S+\beta_2 I)^4}\right] v_1 v_2^2 +$$

$6\left[\frac{\gamma_1\beta_2(1+\omega-\beta_1 S+\beta_2 I)}{(1+\omega+\beta_1 S+\beta_2 I)^3}\right]v_1v_2v_3+6\left[\frac{\gamma_1\beta_2^2 SZ}{(1+\omega+\beta_1 S+\beta_2 I)^4}\right]v_2^3+6\left[\frac{-\gamma_1\beta_2^2 S}{(1+\alpha+\beta_1 S+\beta_2 I)^3}\right]v_2^2v_3$

$$\begin{aligned}d_{21}=&6[\frac{\gamma_2\beta_1^3 IZ}{(1+\omega+\beta_1 S+\beta_2 I)^4}]v_1^3+6[-\frac{\gamma_2\beta_1^2 Z(1+\omega+\beta_1 S-2\beta_2 I)}{(1+\omega+\beta_1 S+\beta_2 I)^4}]v_1^2v_2+6[-\frac{\gamma_2\beta_1^2 I}{(1+\omega+\beta_1 S+\beta_2 I)^3}]v_1^2v_3\\&+6[-\frac{\gamma_2\beta_1\beta_2 Z(2(1+\omega+\beta_1 S)-\beta_2 I)}{(1+\omega+\beta_1 S+\beta_2 I)^4}]v_1v_2^2+6[\frac{\gamma_2\beta_1(1+\omega+\beta_1 S-\beta_2 I)}{(1+\omega+\beta_1 S+\beta_2 I)^3}]v_1v_2v_3\\&+6[-\frac{\gamma_2\beta_2 Z(1+\omega+\beta_1 S)}{(1+\omega+\beta_1 S+\beta_2 I)^4}]v_2^3+6[\frac{\gamma_2\beta_2(1+\omega+\beta_1 S)}{(1+\omega+\beta_1 S+\beta_2 I)^3}]v_2^2v_3\end{aligned}$$

$$\begin{aligned}d_{31}=&6\left[-\frac{\beta_1^2 Z(e_2\gamma_2\beta_1 I-(1+\omega+\beta_2 I)e_1\gamma_1}{(1+\omega+\beta_2 S+\beta_2 I)^4}\right]v_1^3+6\left[\frac{\beta_2 Z(e_1\gamma_1\beta_2(1+\omega-2\beta_1 S+\beta_2 I)+e\gamma_2\beta_1(2(1+\omega+\beta_1 S)-\beta_2 I))}{(1+\omega+\beta_1 S+\beta_2 I)^4}\right]v_1v_2^2\\&+6\left[\frac{\beta_1 Z(e_1\gamma_1\beta_2(2(1+\omega+\beta_2 I)-\beta_1 S)+e_2\gamma_2\beta_1(1+\omega+\beta_1 S-2\beta_2 I)}{(1+w+\beta_2 S+\beta_2 I)^4}\right]v_1^2v_2+6\left[\frac{\beta_1(e_2\gamma_2\beta_1 I-(1+\omega+\beta_2 I)e_1\gamma_1)}{(1+w+\beta_2 S+\beta_2 I)^3}\right]v_1^2v_3\\&-6[\frac{e_1\gamma_1\beta_2(1+\omega-\beta_1 S+\beta_2 I)+e_2\gamma_2\beta_1(1+\omega+\beta_1 S-\beta_2 I)}{(1+\omega+\beta_1 S+\beta_2 I)^3}]v_1v_2v_3+6[-\frac{\beta_2^2 Z(e_1\gamma_1\beta_2 S-e_2\gamma_2(1+\omega+\beta_1 S))}{(1+\omega+\beta_1 S+\beta_2 I)^4}]v_2^3\\&+6\left[\frac{\beta_2\left(e_1\gamma_1\beta_2 S-e_2\gamma_2(1+\omega+\beta_1 S)\right)}{(1+\omega+\beta_1 S+\beta_2 I)^3}\right]v_2^2v_3.\end{aligned}$$

Theorem 8.1. System (1) undergoes a transcritical bifurcation at E_1 when the parameter θ_1 passes into the value $\theta_1^*=\mu k$.

Proof. By using the $J(E_1)$ which given in eq.(9), system (1) has the Jacobian matrix at E_1 and $\theta_1=\theta_1^*$, which represents as $J(E_1,\theta_1^*)$

$$J(E_1,\theta_1^*)=\begin{bmatrix}-r & -k\left(\frac{r}{k}+\mu\right) & \frac{-k\gamma_1}{1+\omega+k\beta_1}\\ 0 & 0 & 0\\ 0 & 0 & \frac{ke_1\gamma_1}{1+\omega+k\beta_1}-\theta_2\end{bmatrix}$$

Obviously, $J(E_1,\theta_1^*)$ possess zero eigenvalue $(\lambda_{12}=0)$ and so E_1 is a non-hyperbolic point. Now, let $\boldsymbol{V}^{[1]}=\left(v_1^{[1]},v_2^{[1]},v_3^{[1]}\right)^T$ and $\boldsymbol{\varphi}^{[1]}=\left(\varphi_1^{[1]},\varphi_2^{[1]},\varphi_3^{[1]}\right)^T$ represent the eigenvectors that corresponding to λ_{12} of $J(E_1,\theta_1^*)$ and $J^T(E_1,\theta_1^*)$. Simple calculations yield $\boldsymbol{V}^{[1]}=(\eta_1 v_2^{[1]},v_2^{[1]},0)^T$ and $\boldsymbol{\varphi}^{[1]}=(0,\varphi_2^{[1]},0)^T$, where $\eta_1=-\frac{r+\mu k}{r}<0$. By using the above Mathematical expressions:

$\boldsymbol{G}_{\theta_1}(\boldsymbol{X},\theta_1)=(0,-I,0)^T\Rightarrow\boldsymbol{G}_{\theta_1}(E_1,\theta_1^*)=(0,0,0)^T\Rightarrow\left(\boldsymbol{\varphi}^{[1]}\right)^T\boldsymbol{G}_{\theta_1}(E_1,\theta_1^*)=0.$

$D\boldsymbol{G}_{\theta_1}(E_1,\theta_1^*)\,\boldsymbol{V}^{[1]}=\left(0,-v_2^{[1]},0\right)^T\Rightarrow\left(\boldsymbol{\varphi}^{[1]}\right)^T\left(D\boldsymbol{G}_{\theta_1}(E_1,\theta_1^*)\,\boldsymbol{V}^{[1]}\right)=-\varphi_2^{[1]}v_2^{[1]}\neq 0.$

Furthermore, utilizing eq. (41) results in

$$\left(\boldsymbol{\varphi}^{[1]}\right)^T\left[D^2\boldsymbol{G}(E_1,\theta_1^*)\left(\boldsymbol{V}^{[1]},\boldsymbol{V}^{[1]}\right)\right]=2\mu\eta_1\varphi_2^{[1]}\left(v_2^{[1]}\right)^2\neq 0.$$

Therefore, by Sotomayor's theorem, the system (1) undergoes a transcritical bifurcation around

E_1 at $\theta_1 = \theta_1^*$.

Theorem 8.2. System (1) undergoes a transcritical bifurcation at E_2 when the parameter θ_2 passes into $\theta_2^* = \frac{e_1\gamma_1\bar{S}+e_2\gamma_2\bar{I}}{1+\omega+\beta_1\bar{S}+\beta_2\bar{I}}$ and provided that the following condition is met

$$\left(\frac{((1+\omega+\beta_2\bar{I})e_1\gamma_1-e_2\gamma_2\beta_1\bar{I})\tau_1+((1+\omega+\beta_1\bar{S})e_2\gamma_2-e_1\gamma_1\beta_2\bar{S})\tau_2}{(1+\omega+\beta_1\bar{S}+\beta_2\bar{I})^2}\right) \neq 0 \qquad (43)$$

Otherwise, system (1) undergoes a pitchfork bifurcation at E_2 provided that the following condition is met

$$(\beta_1\tau_1^2(e_2\gamma_2\beta_1\bar{I} - (1+\omega+\beta_2\bar{I})e_1\gamma_1) - (e_1\gamma_1\beta_2(1+\omega-\beta_1\bar{S}+\beta_2\bar{I}) + e_2\gamma_2\beta_1(1+\omega+\beta_1\bar{S}-\beta_2\bar{I}))\tau_1\tau_2 + \beta_2\tau_2^2(e_1\gamma_1\beta_2\bar{S} - e_2\gamma_2(1+\omega+\beta_1\bar{S}))) \neq 0. \qquad (44)$$

Proof. By using the $J(E_2)$ which given in eq.(12), system (1) has the Jacobian matrix at E_2 and $\theta_2 = \theta_2^*$, which represents as $J(E_2, \theta_2^*)$

$$J(E_2,\theta_2^*) = \begin{bmatrix} b_{11} & b_{12} & b_{13} \\ b_{21} & 0 & b_{23} \\ 0 & 0 & 0 \end{bmatrix}$$

Where $[b_{ij}]$, for all $i,j = 1,2,3$ are given in eq.(12). Clearly, $J(E_2,\theta_2^*)$ has $\lambda_{23} = 0$, which referred a zero eigenvalue and so E_2 is a non-hyperbolic point.

Now, let $\boldsymbol{V}^{[2]} = \left(v_1^{[2]}, v_2^{[2]}, v_3^{[2]}\right)^T$ and $\boldsymbol{\varphi}^{[2]} = \left(\varphi_1^{[2]}, \varphi_2^{[2]}, \varphi_3^{[2]}\right)^T$ represent the eigenvectors that corresponding to λ_{23} of $J(E_2,\theta_2^*)$ and $J^T(E_2,\theta_2^*)$. Simple calculations yield $\boldsymbol{V}^{[2]} = (\tau_1 v_3^{[2]}, \tau_2 v_3^{[2]}, v_3^{[2]})^T$ and $\boldsymbol{\varphi}^{[2]} = (0,0,\varphi_3^{[2]})^T$, where $\tau_1 = \frac{-b_{23}}{b_{21}} > 0$ and $\tau_2 = \frac{b_{11}b_{23}-b_{13}b_{21}}{b_{12}b_{21}} < 0$.

By using the above Mathematical expressions

$$\boldsymbol{G}_{\theta_2}(\boldsymbol{X},\theta_2) = (0,0,-Z)^T \Rightarrow \boldsymbol{G}_{\theta_2}(E_2,\theta_2^*) = (0,0,0)^T \Rightarrow \left(\boldsymbol{\varphi}^{[2]}\right)^T \boldsymbol{G}_{\theta_2}(E_2,\theta_2^*) = 0.$$

$$D\boldsymbol{G}_{\theta_2}(E_2,\theta_2^*)\,\boldsymbol{V}^{[2]} = \left(0,0,-v_3^{[2]}\right)^T \Rightarrow \left(\boldsymbol{\varphi}^{[2]}\right)^T\left(D\boldsymbol{G}_{\theta_2}(E_2,\theta_2^*)\,\boldsymbol{V}^{[2]}\right) = -\varphi_3^{[2]}v_3^{[2]} \neq 0.$$

Furthermore, utilizing eq. (41) results in

$$\left(\boldsymbol{\varphi}^{[2]}\right)^T\left[D^2\boldsymbol{G}(E_2,\theta_2^*)\left(\boldsymbol{V}^{[2]},\boldsymbol{V}^{[2]}\right)\right] = 2\left(\frac{((1+\omega+\beta_2\bar{I})e_1\gamma_1-e_2\gamma_2\beta_1\bar{I})\tau_1+((1+\omega+\beta_1\bar{S})e_2\gamma_2-e_1\gamma_1\beta_2\bar{S})\tau_2}{(1+\omega+\beta_1\bar{S}+\beta_2\bar{I})^2}\right)\varphi_3^{[2]}\left(v_3^{[2]}\right)^2.$$

Therefore, by Sotomayor's theorem, the system (1) undergoes a transcritical bifurcation around E_2 at $\theta_2 = \theta_2^*$, as long as condition (43) is valid.

In case the condition (43) is not fulfilled, then using eq. (42) it is determined that

$\left(\boldsymbol{\varphi}^{[2]}\right)^T\left(D^3\boldsymbol{G}(E_2,\theta_2^*)\left(\boldsymbol{V}^{[2]},\boldsymbol{V}^{[2]},\boldsymbol{V}^{[2]}\right)\right)=\frac{6\,\varphi_3^{[2]}\left(v_3^{[2]}\right)^3}{(1+\omega+\beta_1\bar{S}+\beta_2\bar{I})^3}\left[\beta_1\tau_1^2(e_2\gamma_2\beta_1\bar{I}-(1+\omega+\beta_2\bar{I})e_1\gamma_1)-(e_1\gamma_1\beta_2(1+\omega-\beta_1\bar{S}+\beta_2\bar{I})+e_2\gamma_2\beta_1(1+\omega+\beta_1\bar{S}-\beta_2\bar{I}))\tau_1\tau_2+\beta_2\tau_2^2(e_1\gamma_1\beta_2\bar{S}-e_2\gamma_2(1+\omega+\beta_1\bar{S}))\right].$

This indicates that a pitchfork bifurcation can occurred as long as condition (44) is valid. If condition (44) is not fulfilled, then no any type of local bifurcation occurs.

Theorem 8.3. System (1) undergoes a transcritical bifurcation at E_3 when the parameter μ passes into $\mu^*=\frac{1}{\hat{S}}\left(\frac{\gamma_2\hat{Z}}{1+\omega+\beta_1\hat{S}}+\theta_1\right)$ and provided that the following condition is met

$$\left(\left(\mu^*+\frac{\gamma_2\beta_1\hat{Z}}{(1+\omega+\beta_1\hat{S})^2}\right)\delta_1-\frac{\gamma_2\,\delta_2}{1+\omega+\beta_1\hat{S}}+\frac{\gamma_2\beta_2\hat{Z}}{\left(1+\omega+\beta_1\hat{S}\right)^2}\right)\neq 0 \tag{45}$$

Otherwise, system (1) undergoes a pitchfork bifurcation provided that the following condition is met

$$\left((\beta_1\delta_1+\beta_2)((1+\omega+\beta_1\hat{S})\delta_2-\beta_1^2\hat{Z}\delta_1)-\beta_2\hat{Z}\right)\neq 0 \tag{46}$$

Proof. By using the $J(E_3)$ which given in eq.(15), system (1) has the Jacobian matrix at E_3 and $\mu=\mu^*$, which represents as $J(E_3,\mu^*)$

$$J(E_3,\mu^*)=\begin{bmatrix}c_{11} & c_{12} & c_{13}\\ 0 & 0 & 0\\ c_{31} & c_{32} & 0\end{bmatrix}$$

Where $[c_{ij}]$, for all $i,j=1,2,3$ are given in eq.(15). Clearly, $J(E_3,\mu^*)$ has $\lambda_{32}=0$, which referred a zero eigenvalue and so E_3 is a non-hyperbolic point.

Now, let $\boldsymbol{V}^{[3]}=\left(v_1^{[3]},v_2^{[3]},v_3^{[3]}\right)^T$ and $\boldsymbol{\varphi}^{[3]}=\left(\varphi_1^{[3]},\varphi_2^{[3]},\varphi_3^{[3]}\right)^T$ represent the eigenvectors that corresponding to λ_{32} of $J(E_3,\mu^*)$ and $J^T(E_3,\mu^*)$. Simple calculations yield $\boldsymbol{V}^{[3]}=(\delta_1 v_2^{[3]},v_2^{[3]},\delta_2 v_2^{[3]})^T$ and $\boldsymbol{\varphi}^{[3]}=(0,\varphi_2^{[3]},0)^T$, where $\delta_1=\frac{-c_{32}}{c_{31}}<0$ and $\delta_2=\frac{c_{11}c_{32}-c_{12}c_{31}}{c_{13}c_{31}}$. By using the above Mathematical expressions

$\boldsymbol{G}_\mu(\boldsymbol{X},\mu)=(-SI,SI,0)^T\Rightarrow\boldsymbol{G}_\mu(E_3,\mu^*)=(0,0,0)^T\Rightarrow\left(\boldsymbol{\varphi}^{[3]}\right)^T\boldsymbol{G}_\mu(E_3,\mu^*)=0.$

$D\boldsymbol{G}_\mu(E_3,\mu^*)\,\boldsymbol{V}^{[3]}=\left(-\hat{S}\,v_2^{[3]},\hat{S}\,v_2^{[3]},0\right)^T\Rightarrow\left(\boldsymbol{\varphi}^{[3]}\right)^T\left(D\boldsymbol{G}_\mu(E_3,\mu^*)\,\boldsymbol{V}^{[3]}\right)=\hat{S}\,\varphi_2^{[3]}v_2^{[3]}\neq 0.$

Furthermore, utilizing eq. (41) results in

$$\left(\boldsymbol{\varphi}^{[3]}\right)^T\left[D^2\boldsymbol{G}(E_3,\mu^*)\left(\boldsymbol{V}^{[3]},\boldsymbol{V}^{[3]}\right)\right]=2\varphi_2^{[3]}\left(v_2^{[3]}\right)^2\left(\left(\mu^*+\frac{\gamma_2\beta_1\hat{Z}}{(1+\omega+\beta_1\hat{S})^2}\right)\delta_1-\frac{\gamma_2\,\delta_2}{1+\omega+\beta_1\hat{S}}+\frac{\gamma_2\beta_2\hat{Z}}{\left(1+\omega+\beta_1\hat{S}\right)^2}\right).$$

Therefore, by Sotomayor's theorem, the system (1) undergoes a transcritical bifurcation around E_3 at $\mu=\mu^*$, as long as condition (45) is valid.

If condition (45) is not fulfilled, then using eq. (42) it is determined that

$$\left(\boldsymbol{\varphi}^{[3]}\right)^T\left(D^3\boldsymbol{G}(E_3,\mu^*)\left(\boldsymbol{V}^{[3]},\boldsymbol{V}^{[3]},\boldsymbol{V}^{[3]}\right)\right)=\frac{6\gamma_2\varphi_2^{[3]}\left(v_2^{[3]}\right)^3}{\left(1+\omega+\beta_1\hat{S}\right)^3}\left((\beta_1\delta_1+\beta_2)\left((1+\omega+\beta_1\hat{S})\delta_2-\beta_1^2\hat{Z}\delta_1\right)-\beta_2\hat{Z}\right).$$

This indicates that a pitchfork bifurcation can occurred as long as condition (46) is valid. If condition (46) is not fulfilled, then no any type of local bifurcation occurs.

Theorem 8.4. System (1) undergoes a saddle-node bifurcation at E_4 when the parameter r passes into $r^*=\frac{k}{S^*a_{23}(a_{31}-a_{32})}[a_{13}B_1+a_{23}B_2]$, where $B_1=(a_{21}a_{32}-a_{22}a_{31})>0, B_2=\frac{\gamma_1\beta_2S^*Z^*a_{31}}{(1+\omega+\beta_1S^*+\beta_2I^*)^2}-\left(\mu S^*a_{31}+\frac{\gamma_1\beta_1S^*Z^*a_{32}}{(1+\omega+\beta_1S^*+\beta_2I^*)^2}\right)$ provided that conditions (21) and (23) with the following conditions are met

$$a_{32}<a_{31} \tag{47}$$

$$\mu S^*a_{31}+\frac{\gamma_1\beta_1S^*Z^*a_{32}}{(1+\omega+\beta_1S^*+\beta_2I^*)^2}<\frac{\gamma_1\beta_2S^*Z^*a_{31}}{(1+\omega+\beta_1S^*+\beta_2I^*)^2} \tag{48}$$

$$\iota_1\varphi_3^{[4]}{c_{11}}^*+\iota_2\varphi_3^{[4]}{c_{21}}^*+\varphi_3^{[4]}{c_{31}}^*\neq 0 \tag{49}$$

where a_{ij} for all $i,j=1,2,3$ are given in eq. (20).

Proof. By using the $J(E_4)$ which given in eq. (19), system (1) has the Jacobian matrix at E_4 and $r=r^*$, which represents as $J(E_4,r^*)=\left[{a_{ij}}^*\right]$, where ${a_{ij}}^*=a_{ij}$; $\forall\, i,j=1,2,3$.

Direct calculation shows that $A_3^*=0$ in the characteristic equation which given in eq. (20) and then E_4 becomes a non-hyperbolic equilibrium point with $\lambda^*=0$.

Now, let $\boldsymbol{V}^{[4]}=\left(v_1^{[4]},v_2^{[4]},v_3^{[4]}\right)^T$ and $\boldsymbol{\varphi}^{[4]}=\left(\varphi_1^{[4]},\varphi_2^{[4]},\varphi_3^{[4]}\right)^T$ represent the eigenvectors that corresponding to λ^* of $J(E_4,r^*)$ and $J^T(E_4,r^*)$. Simple calculations yield $\boldsymbol{V}^{[4]}=(\varepsilon_1v_3^{[4]},\varepsilon_2v_3^{[4]},v_3^{[4]})^T$ and $\boldsymbol{\varphi}^{[3]}=(\iota_1\varphi_3^{[4]},\iota_2\varphi_3^{[4]},\varphi_3^{[4]})^T$, where

$$\varepsilon_1=\frac{a_{12}(a_{11}a_{23}-a_{13}a_{21})+a_{13}(a_{12}a_{21}-a_{11}a_{22})}{a_{11}(a_{11}a_{22}-a_{12}a_{21})},\ \varepsilon_2=\frac{(a_{13}a_{21}-a_{11}a_{23})}{(a_{11}a_{22}-a_{12}a_{21})},$$

$\iota_1 = \frac{a_{21}(a_{11}a_{32}-a_{12}a_{31})+a_{31}(a_{11}a_{22}-a_{12}a_{21})}{a_{11}(a_{11}a_{22}-a_{12}a_{21})}$ $and\ \iota_2 = \frac{(a_{12}a_{31}-a_{11}a_{32})}{(a_{11}a_{22}-a_{12}a_{21})}$. By using the above Mathematical expressions

$\boldsymbol{G}_r(\boldsymbol{X}, r) = \left(S\left(1-\frac{S+I}{K}\right), 0{,}0\right)^T \Rightarrow \boldsymbol{G}_r(E_4, r^*) = \left(S^*\left(1-\frac{S^*+I^*}{K}\right), 0{,}0\right)^T \Rightarrow \left(\boldsymbol{\varphi}^{[4]}\right)^T \boldsymbol{G}_r(E_4, r^*) = \iota_1 S^*\left(1-\frac{S^*+I^*}{K}\right)\varphi_3^{[4]} \neq 0.$

According to Sotomayor's theorem a first condition of the saddle-node bifurcation is occurred. Moreover, since

$$D^2\boldsymbol{G}(E_4, r^*)\left(\boldsymbol{V}^{[4]}, \boldsymbol{V}^{[4]}\right) = \left[c_{ij}{}^*\right]_{3\times 1},$$

Here,

$c_{11}{}^* = 2\left[-\frac{r^*}{k} + \frac{\gamma_1\beta_1 Z^*(1+\omega+\beta_2 I^*)}{(1+\omega+\beta_1 S^*+\beta_2 I^*)^3}\right]\left(\varepsilon_1 v_3^{[4]}\right)^2 + 2\left[-\left(\frac{r^*}{k}+\mu\right) + \frac{\gamma_1\beta_2 Z^*(1+\omega-\beta_1 S^*+\beta_2 I^*)}{(1+\omega+\beta_1 S^*+\beta_2 I^*)^3}\right]\varepsilon_1\varepsilon_2\left(v_3^{[4]}\right)^2 + 2\left[-\frac{\gamma_1(1+\omega+\beta_2 I^*)}{(1+\omega+\beta_1 S^*+\beta_2 I^*)^2}\right]\varepsilon_1\left(v_3^{[4]}\right)^2 + 2\left[-\frac{\gamma_1\beta_2^2 S^* Z^*}{(1+\omega+\beta_1 S^*+\beta_2 I^*)^3}\right]\left(\varepsilon_2 v_3^{[4]}\right)^2 + 2\left[\frac{\gamma_1\beta_2 S^*}{(1+\omega+\beta_1 S^*+\beta_2 I^*)^2}\right]\varepsilon_2\left(v_3^{[4]}\right)^2.$

$$c_{21}{}^* = 2\left[-\frac{\gamma_2\beta_1^2 I^* Z^*}{(1+\omega+\beta_1 S^*+\beta_2 I^*)^3}\right]\left(\varepsilon_1 v_3^{[4]}\right)^2 + 2\left[\mu + \frac{\gamma_2\beta_1 Z^*(1+\omega+\beta_1 S^*-\beta_2 I^*)}{(1+\omega+\beta_1 S^*+\beta_2 I^*)^3}\right]\varepsilon_1\varepsilon_2\left(v_3^{[4]}\right)^2$$
$$+2\left[\frac{\gamma_2\beta_1 I^*}{(1+\omega+\beta_1 S^*+\beta_2 I^*)^2}\right]\varepsilon_1\left(v_3^{[4]}\right)^2 + 2\left[\frac{\gamma_2\beta_2 Z^*(1+\omega+\beta_1 S^*)}{(1+\omega+\beta_1 S^*+\beta_2 I^*)^3}\right]\left(\varepsilon_2 v_3^{[4]}\right)^2 + 2\left[-\frac{\gamma_2(1+\omega+\beta_1 S^*)}{(1+\omega+\beta_1 S^*+\beta_2 I^*)^2}\right]\varepsilon_2\left(v_3^{[4]}\right)^2$$

$c_{31}{}^* = 2\left[\frac{\beta_1 Z^*(e_2\gamma_2\beta_1 I^* - (1+\omega+\beta_2 I^*)e_1\gamma_1)}{(1+\omega+\beta_1 S^*+\beta_2 I^*)^3}\right]\left(\varepsilon_1 v_3^{[4]}\right)^2 + 2\left[\frac{-Z^*\left(e_1\gamma_1\beta_2(1+\omega-\beta_1 S^*+\beta_2 I^*)+e_2\gamma_2\beta_1(1+\omega+\beta_1 S^*-\beta_2 I^*)\right)}{(1+\omega+\beta_1 S^*+\beta_2 I^*)^3}\right]\varepsilon_1\varepsilon_2\left(v_3^{[4]}\right)^2 + 2\left[\frac{(1+\omega+\beta_2 I^*)e_1\gamma_1 - e_2\gamma_2\beta_1 I^*}{(1+\omega+\beta_1 S^*+\beta_2 I^*)^2}\right]\varepsilon_1\left(v_3^{[4]}\right)^2 + 2\left[\frac{\beta_2 Z^*(e_1\gamma_1\beta_2 S^* - (1+\omega+\beta_1 S^*)e_2\gamma_2}{(1+\omega+\beta_1 S^*+\beta_2 I^*)^3}\right]\left(\varepsilon_2 v_3^{[4]}\right)^2 + 2\left[\frac{(1+\omega+\beta_1 S^*)e_2\gamma_2 - e_1\gamma_1\beta_2 S^*}{(1+\omega+\beta_1 S^*+\beta_2 I^*)^2}\right]\varepsilon_2\left(v_3^{[4]}\right)^2.$

Furthermore, utilizing eq. (41) results in

$$\left(\boldsymbol{\varphi}^{[4]}\right)^T\left[D^2\boldsymbol{G}(E_4, r^*)\left(\boldsymbol{V}^{[4]}, \boldsymbol{V}^{[4]}\right)\right] = \iota_1\varphi_3^{[4]}c_{11}{}^* + \iota_2\varphi_3^{[4]}c_{21}{}^* + \varphi_3^{[4]}c_{31}{}^* \neq 0.$$

Therefore, by Sotomayor's theorem, the system (1) undergoes a saddle-node bifurcation around E_4 at $r = r^*$, as long as conditions (47-49) are valid.

9. NUMERICAL ANALYSIS

In this section, the dynamics of system (1) are investigated numerically. The aim is to complete the visualization of the global dynamics of the system, and to discover the effect of changing the values of the parameters on its dynamic behavior. The solutions are analyzed by analyzing time series and phase portraits analyses utilizing MATLAB Program. All the results are use the following initial points $(3,5,7),(5,5,5),(4,7,6),(6,2,5),(8,6,4)$.

The set of presumptive parameter values, which given in table (1), are utilized.

Table 1: Presumptive sets of parameters:

Parameters	r	k	μ	γ_1	ω	β_1	β_2	γ_2	θ_1	e_1	e_2	θ_2
Values	2	10	0.02	0.2	2	0.6	0.4	0.25	0.08	0.4	0.4	0.1

Furthermore, the blue points refer to the initial points, whilst the red point refers to the final state of the solution. It is noted that for the values in the table (1), system (1) approaches an interior equilibrium point as illustrated in Figure 1.

Figure 1 shows that system (1) approaches asymptotically to the interior equilibrium point $E_4 = (6.7,2.7,1.7)$ from various initial points.

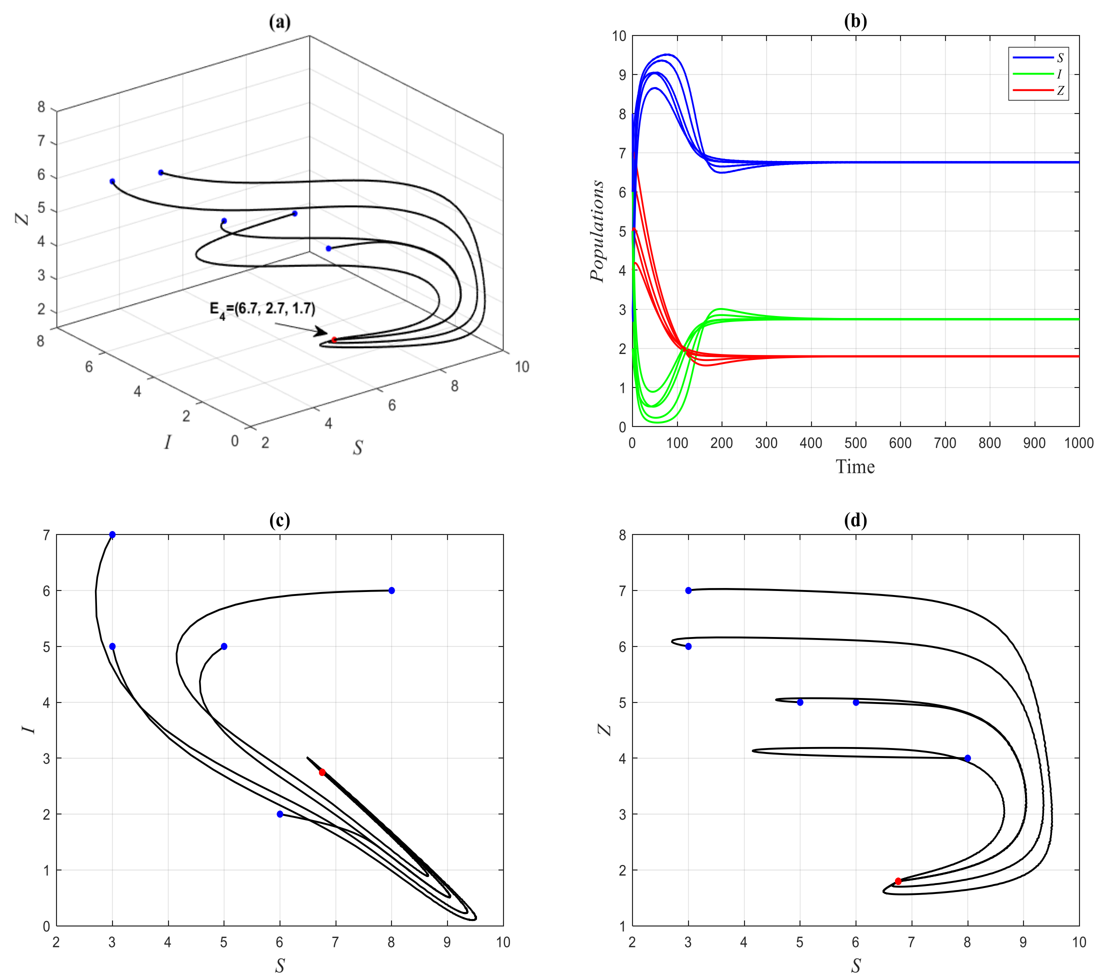

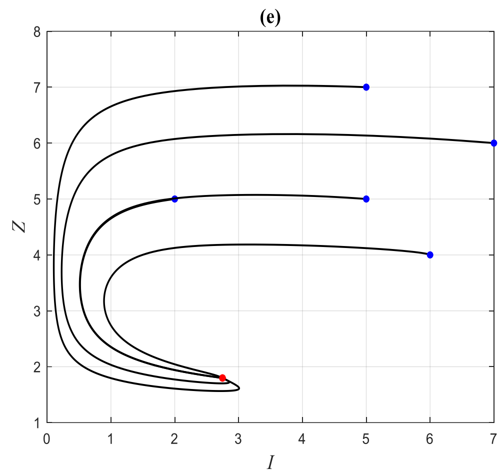

Figure 1. The trajectory of the system (1) utilizing the parameter values in table (1). (a) Illustrates the phase portrait from various initial points. (b) Shows the time series of (a). (c) Illustrates the projection on the $SI-$plane. (d) Illustrates the projection on the $IZ-$plane. (e) Illustrates the projection on the $SZ-$plane.

Now, the impact of changing the parameter r on the dynamic of system (1) refers that when $0 < r \leq 0.29$, the system approaches E_2 in the $SI-$plane from various initial points (see Figure 2). Also, system (1) approaches the interior point E_4 when $0.3 < r$, which is illustrated by Figure 1.

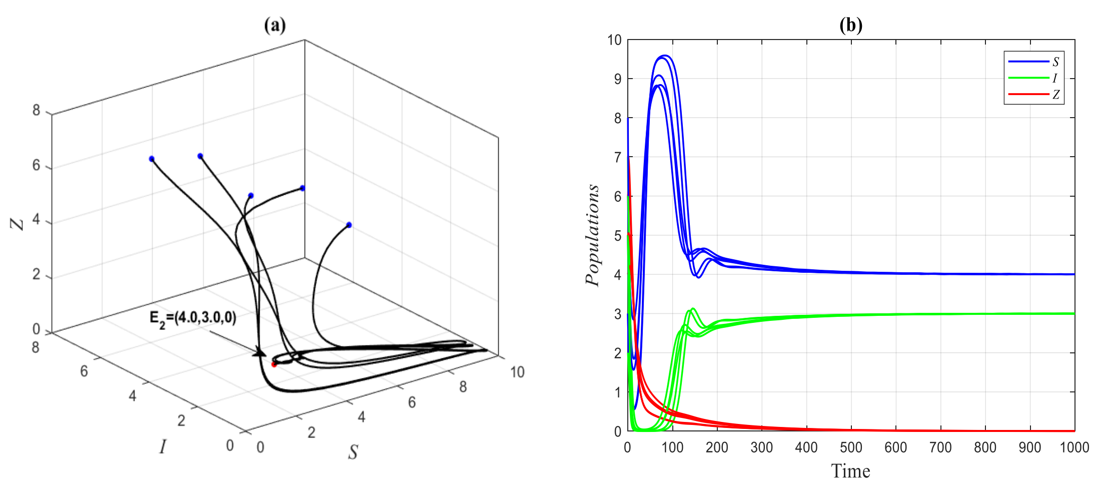

Figure 2. The trajectory of the system (1) utilizing the parameter values in table (1) with different values of r. (a) Illustrates the phase portrait when $r = 0.2$. (b) Shows the time series of (a).

In Figure 3, the effect of varying the parameter k on the dynamic of system (1) discovers that it approaches E_1 when $1 \le k < 4.2$. So, it approaches E_2 in the $SI-$plane when $4.2 \le k < 7.6$. in the range $7.6 \le k < 17$, the trajectory approaches E_4 (see Figure1).The trajectory approaches E_3 in the $SZ-$plane when $17 \le k < 35$. Finally, for $35 \le k$ the trajectory approaches a periodic oscillation in the $SZ-$plane.

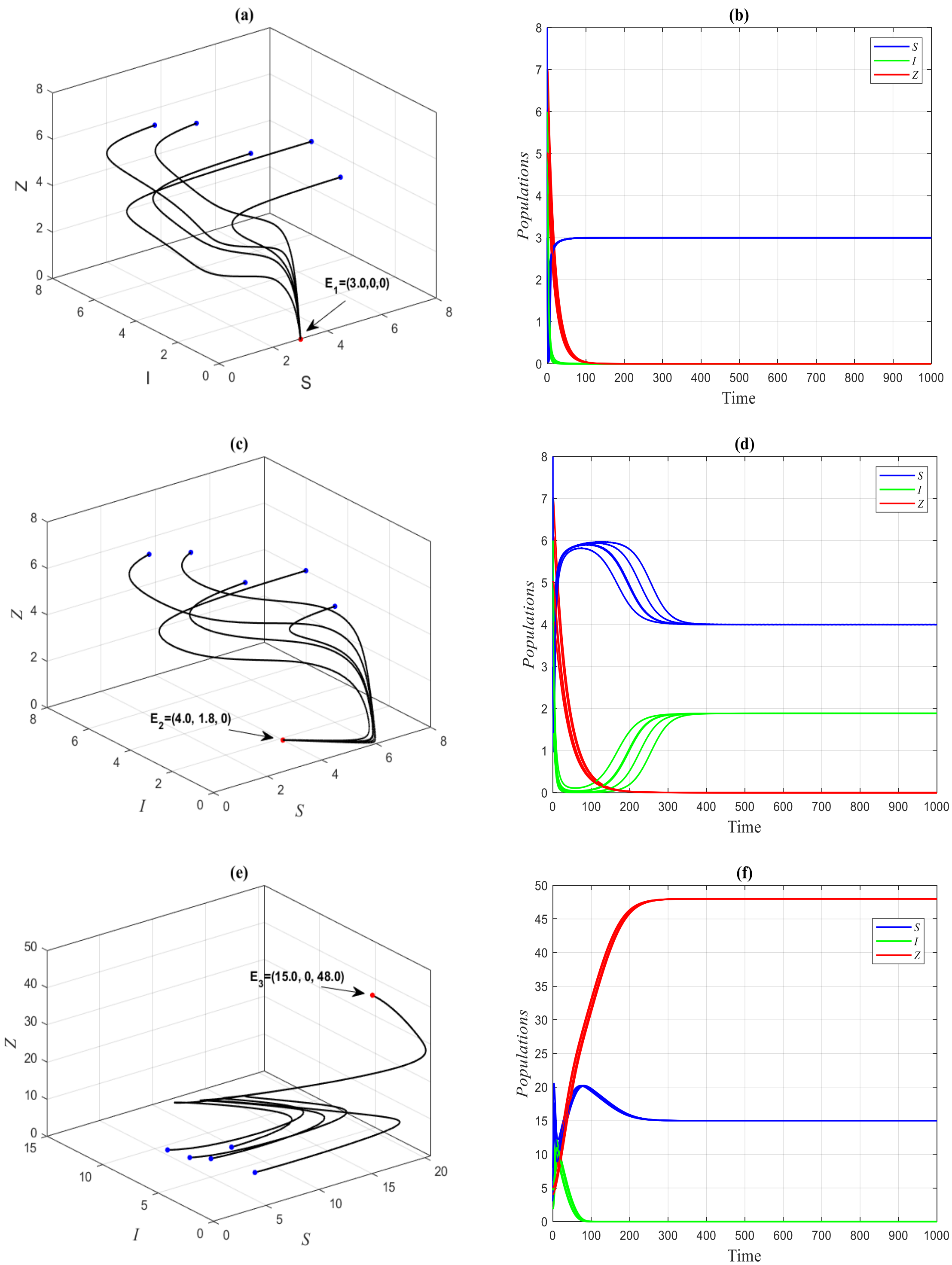

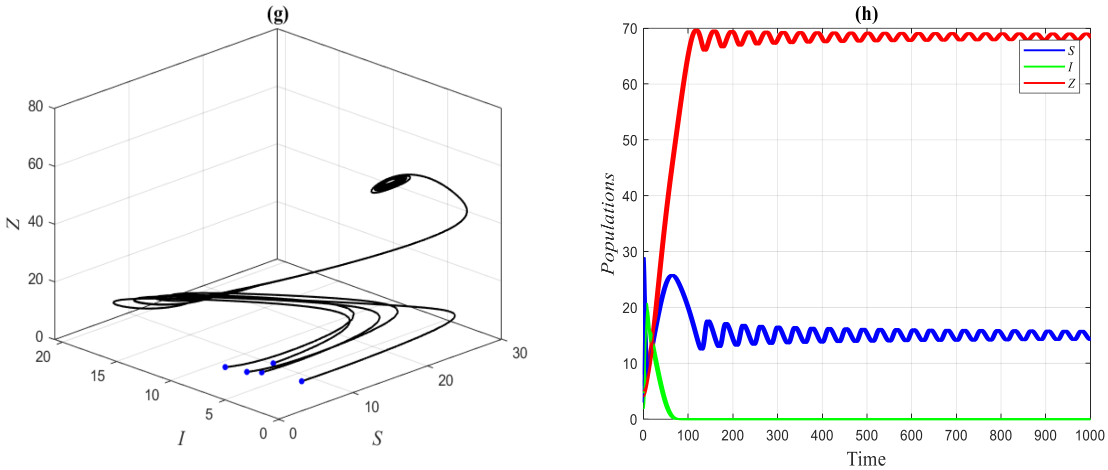

Figure 3. The trajectory of the system (1) utilizing the parameter values in table (1) with different values of k. (a) Illustrates the phase portrait when $k = 3$. (b) Shows the time series of (a). (c) Illustrates the phase portrait when $k = 6$. (d) Shows the time series of (c). (e) Illustrates the phase portrait when $k = 20$. (f) Shows the time series of (e). (g) Illustrates the phase portrait when $k = 35$. (h) Shows the time series of (g).

It is observed that system (1) approaches E_1 when $\mu = 0$ (in the absence of disease), it approaches E_2 in the $SI-$plane when $0 < \mu < 0.01$. In the range $0.01 \leq \mu < 0.3$ the trajectory approaches E_4 (see Figure 1). Again, system (1) approaches E_2 in the $SI-$plane when $0.3 \leq \mu$, (see Figure 4).

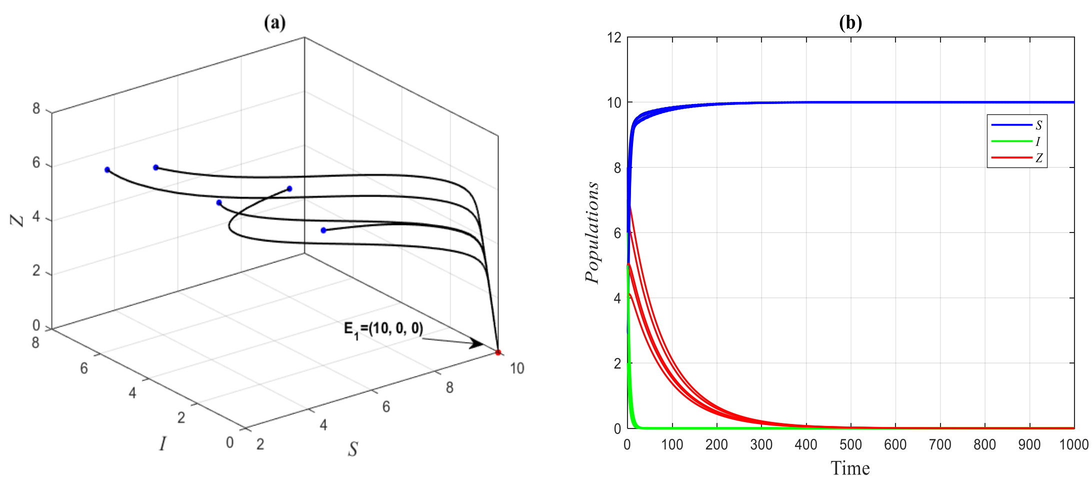

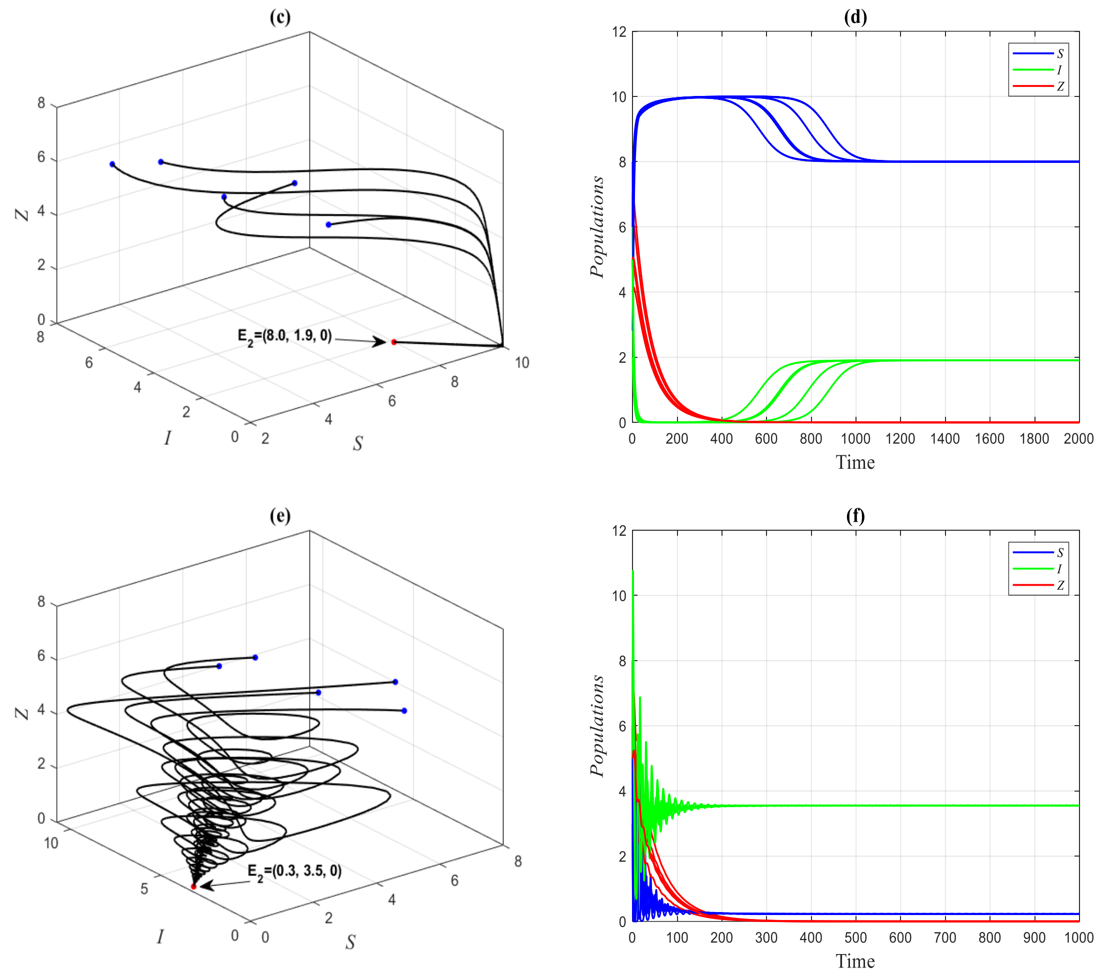

Figure 4. The trajectory of the system (1) utilizing the parameter values in table (1) with different values of μ. (a) Illustrates the phase portrait when $\mu = 0$. (b) Shows the time series of (a). (c) Illustrates the phase portrait when $\mu = 0.01$. (d) Shows the time series of (c). (e) Illustrates the phase portrait when $\mu = 0.35$. (f) Shows the time series of (e).

To explain the impact of changing the parameter ω on the dynamic of system (1) and by utilizing the parameter values in table (1), the impact of wind flow with various values are plot as illustrated in Figure 5. It is note that, system (1) approaches E_3 in the $SZ -$ plane when $0 \leq w < 1$. Also, the trajectory approaches asymptotically E_4 in the range $1 \leq \omega < 3.5$. Moreover, it approaches E_2 in the $SI -$ plane for $3.5 \leq \omega$.

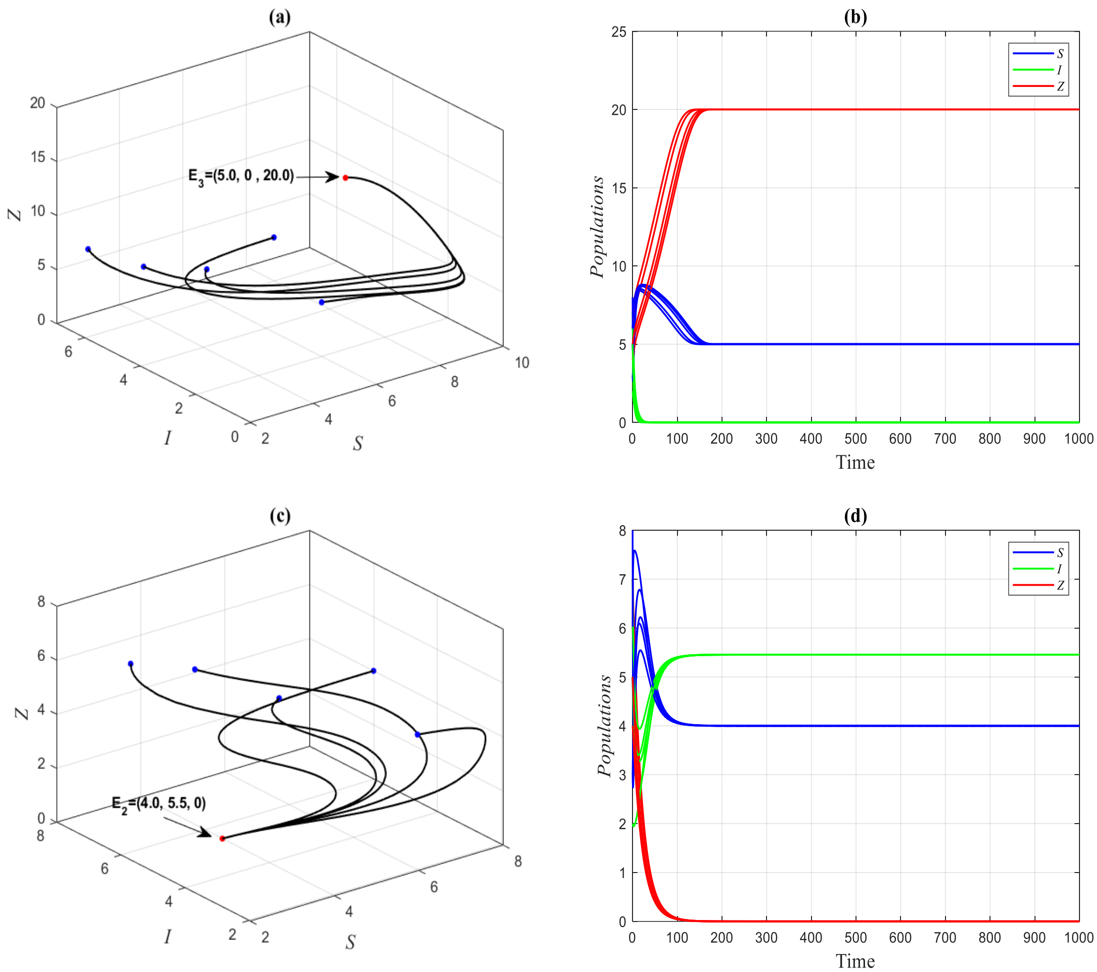

Figure 5. The trajectory of the system (1) utilizing the parameter values in table (1) with different values of ω. (a) Illustrates the phase portrait when $\omega = 0$. (b) Shows the time series of (a). (c) Illustrates the phase portrait when $\omega = 10$. (d) Shows the time series of (c).

In Figure 6, the effect of varying the parameter γ_1 on the dynamic of system (1) discovers that it approaches E_2 in the $SI-$plane when $0 < \gamma_1 < 0.1$. So, it approaches E_4 when $0.1 \le \gamma_1 < 0.3$ (see Figure1). In the range $0.3 \le \gamma_1 < 0.45$, the trajectory approaches E_3 in the $SZ-$plane. Finally, for $0.45 \le \gamma_1$ the trajectory approaches a periodic oscillation in the $SZ-$plane.

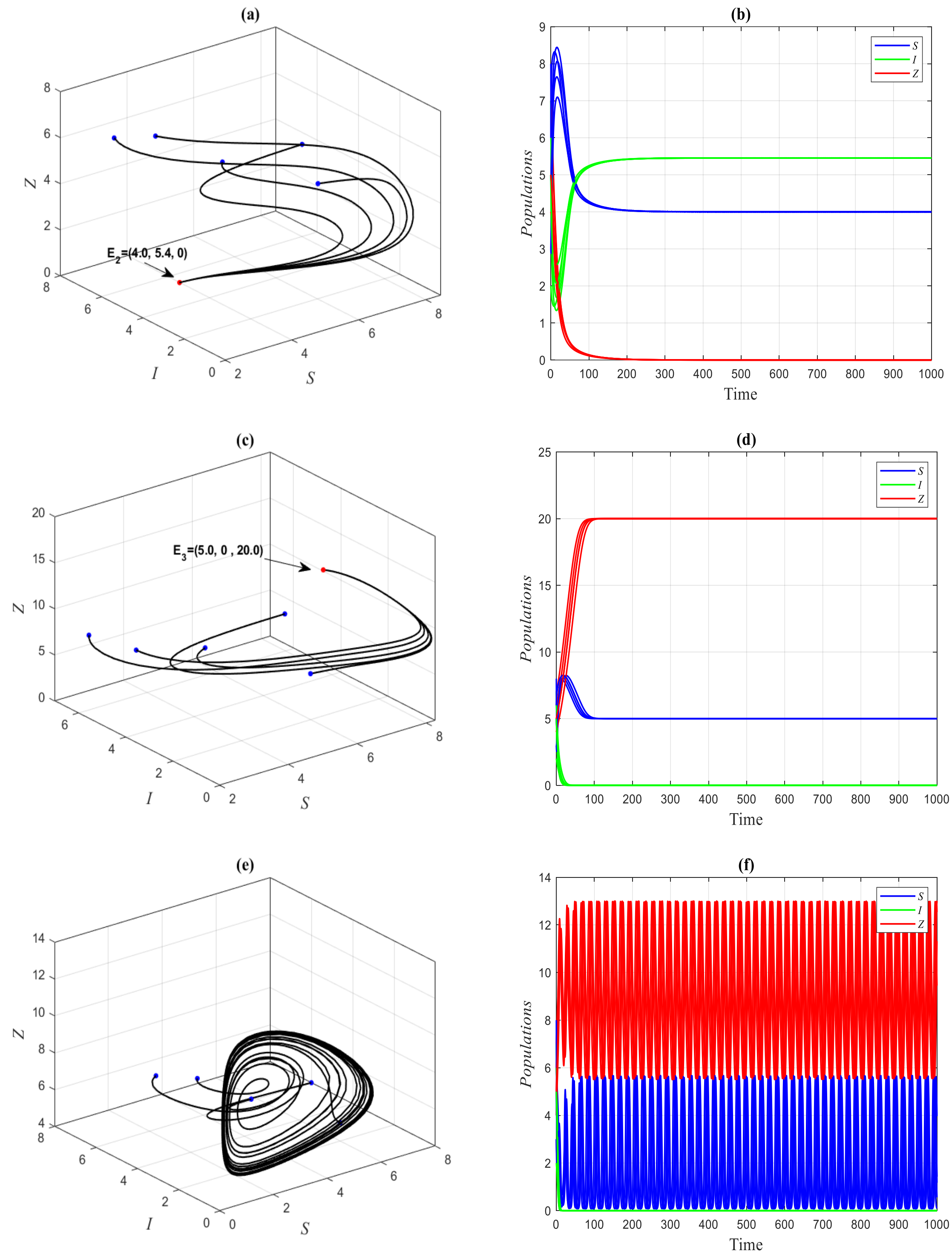
(a)
(b)
(c)
(d)
(e)
(f)
E_2=(4.0, 5.4, 0)
E_3=(5.0, 0 , 20.0)
Z
I
S
Populations
Time
S
I
Z

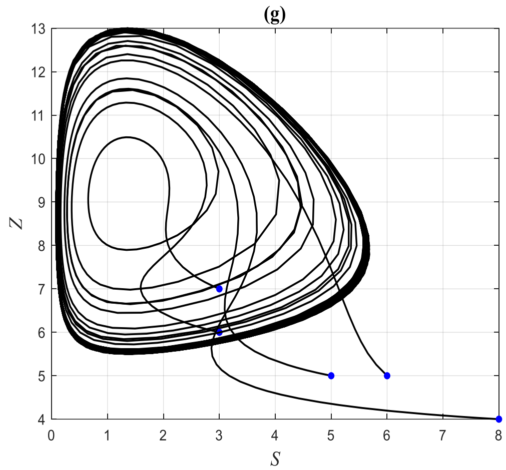

Figure 6. The trajectory of the system (1) utilizing the parameter values in table (1) with different values of γ_1. (a) Illustrates the phase portrait when $\gamma_1 = 0.05$. (b) Shows the time series of (a). (c) Illustrates the phase portrait when $\gamma_1 = 0.3$. (d) Shows the time series of (c). (e) Illustrates the phase portrait when $\gamma_1 = 0.7$. (f) Shows the time series of (e). (g) Illustrates the projection on the $SZ-$plane.

The influence of changing the parameter β_1 on the dynamic of system (1) refers that when $0 < \beta_1 < 0.5$ the trajectory approaches E_3 in the $SZ-$plane as in Figure 7. Moreover, the trajectory approaches E_4 when $0.5 \leq \beta_1$, see Figure 1.

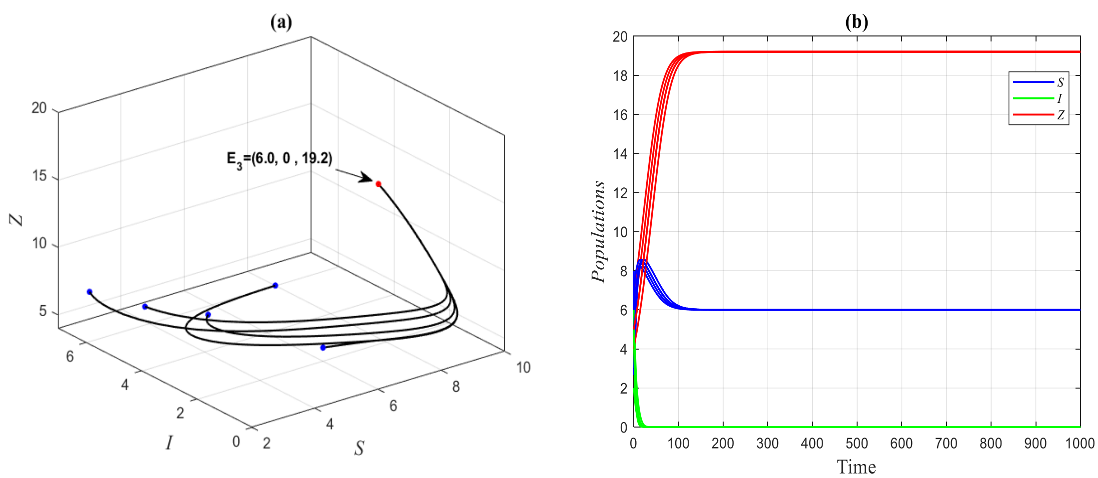

Figure 7. The trajectory of the system (1) utilizing the parameter values in table (1) with different values of β_1. (a) Illustrates the phase portrait when $\beta_1 = 0.3$. (b) Shows the time series of (a).

The influence of changing the parameter β_2 on the dynamic of system (1) refers that when $0 < \beta_2 < 0.7$ the trajectory approaches E_4 as in Figure 1. Furthermore, the trajectory approaches

E_2 in the $SI-$plane when $0.7 \le \beta_2$, see Figure 8.

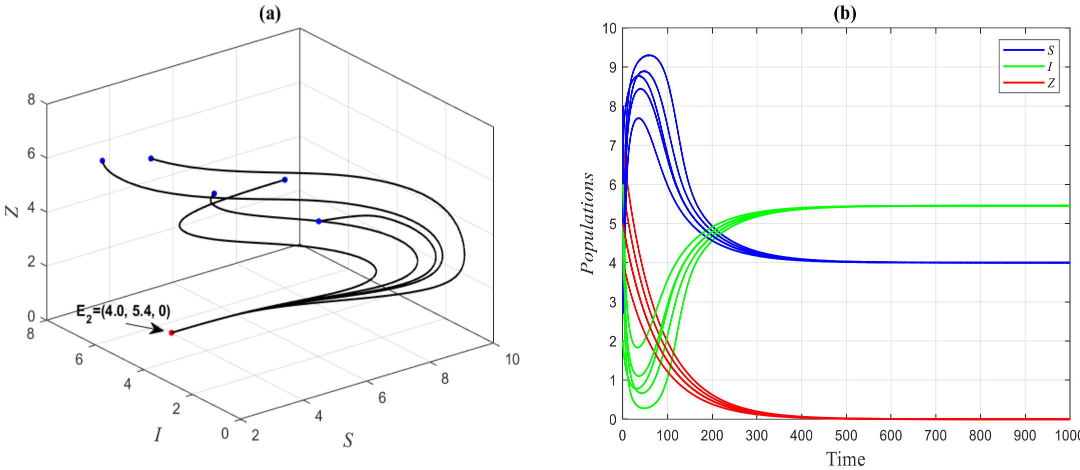

Figure 8. The trajectory of the system (1) utilizing the parameter values in table (1) with different values of β_2. (a) Illustrates the phase portrait when $\beta_2 = 0.8$. (b) Shows the time series of (a).

The impact of varying the parameter γ_2 on the dynamic of system (1) indicates that when $0 < \gamma_2 < 0.2$ the trajectory approaches E_2 in the $SI-$plane as in Figure 9. Furthermore, the trajectory approaches E_4 when $0.2 \le \gamma_2$, see Figure 1.

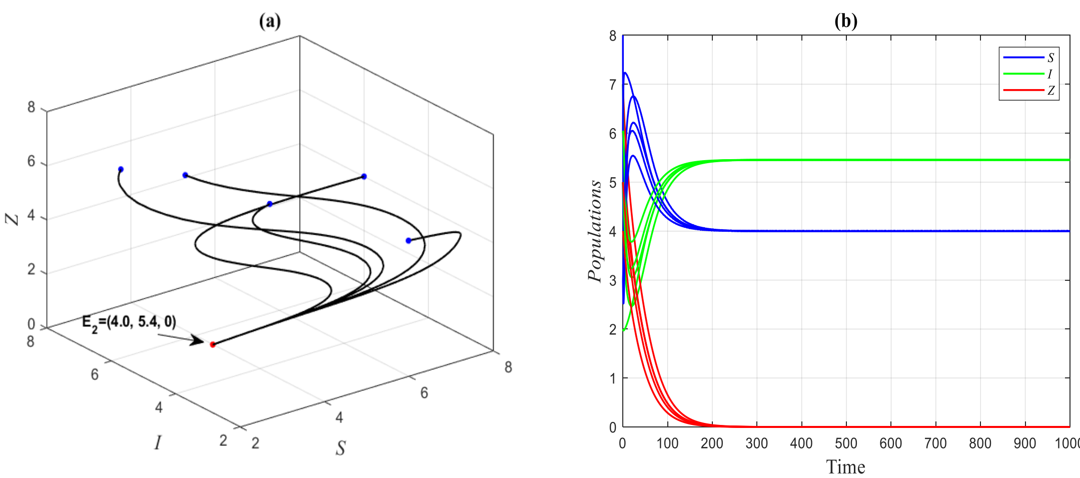

Figure 9. The trajectory of the system (1) utilizing the parameter values in table (1) with different values of γ_2. (a) Illustrates the phase portrait when $\gamma_2 = 0.1$. (b) Shows the time series of (a).

Now, the impact of changing the parameter e_1 on the dynamic of system (1) refers that when $0 < e_1 < 0.3$, the system approaches E_2 in the $SI-$plane from various initial points. Also, system

(1) approaches the interior point E_4 when $0.3 \leq e_1 < 0.5$, which is illustrated by Figure 1. For $0.5 \leq e_1 < 0.9$, it approaches E_3 in the $SZ-$plane, while for $0.9 \leq e_1$, it approaches a periodic oscillation in the $SZ-$plane, see Figure 10.

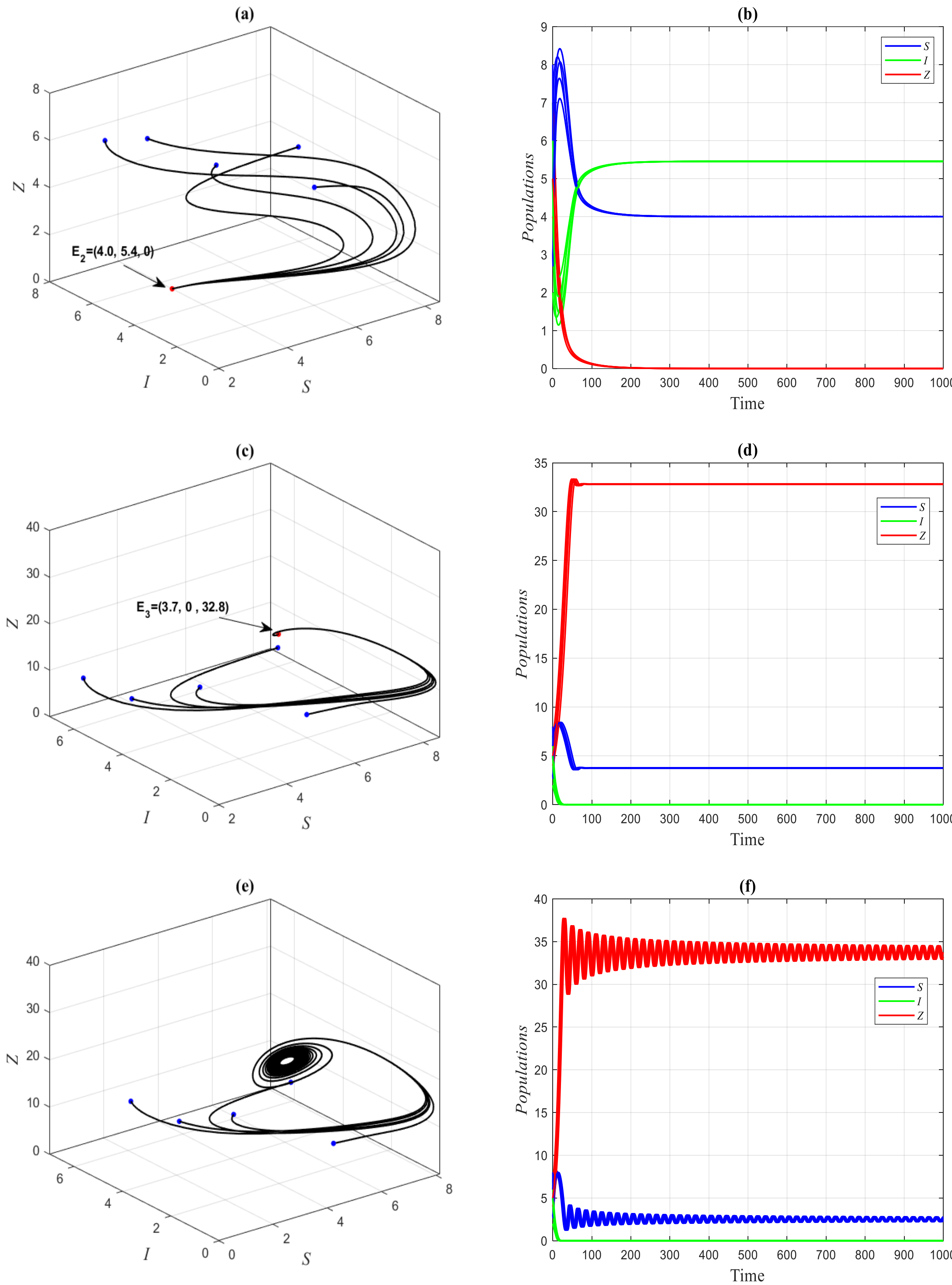

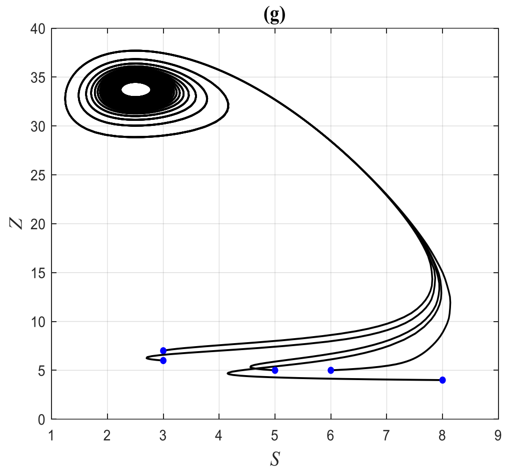

Figure 10. The trajectory of the system (1) utilizing the parameter values in table (1) with different values of e_1. (a) Illustrates the phase portrait when $e_1 = 0.1$. (b) Shows the time series of (a). (c) Illustrates the phase portrait when $e_1 = 07$. (d) Shows the time series of (c). (e) Illustrates the phase portrait when $e_1 = 0.9$. (f) Shows the time series of (e). (g) Illustrates the projection on the $SZ -$ plane.

The impact of varying the parameter θ_1 on the dynamic of system (1) refers that when $0 < \theta_1 < 0.2$ the trajectory approaches E_4 as in Figure 1. So, the trajectory approaches E_1 when $0.2 \leq \theta_1$, see Figure 11.

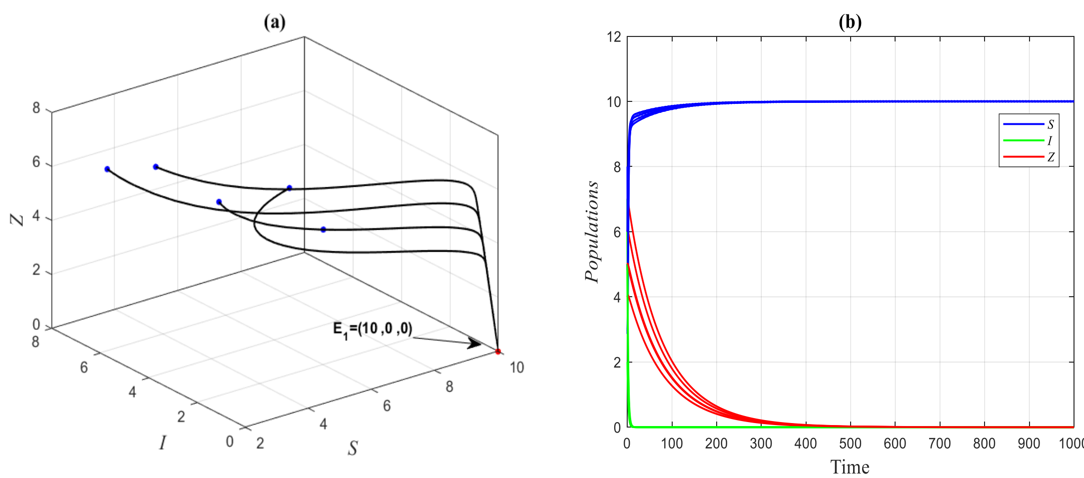

Figure 11. The trajectory of the system (1) utilizing the parameter values in table (1) with different values of θ_1. (a) Illustrates the phase portrait when $\theta_1 = 0.5$. (b) Shows the time series of (a).

In Figure 12, the effect of varying the parameter e_2 on the dynamic of system (1) discovers that it approaches E_2 in the $SI-$plane when $0 < e_2 < 0.35$. So, it approaches E_4 when $0.35 \leq e_2$.

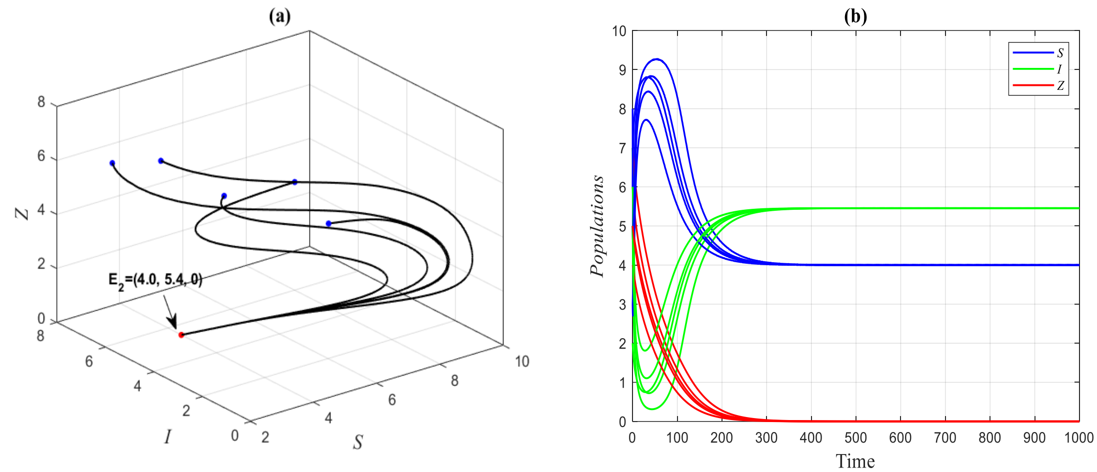

Figure 12. The trajectory of the system (1) utilizing the parameter values in table (1) with different values of e_2. (a) Illustrates the phase portrait when $e_2 = 0.2$. (b) Shows the time series of (a).

Finally, the impact of varying the parameter θ_2 on the dynamic of system (1) refers that when $0 < \theta_2 < 0.05$ the trajectory approaches a periodic oscillation in the $SZ-$plane. Furthermore, the trajectory approaches E_3 in the $SZ-$plane when $0.05 \leq \theta_2 < 0.1$, while it approaches E_4 when $0.1 \leq \theta_2 < 0.2$. moreover, for $0.2 \leq \theta_2$ the trajectory approaches E_2 in the $SI-$plane see Figure 13.

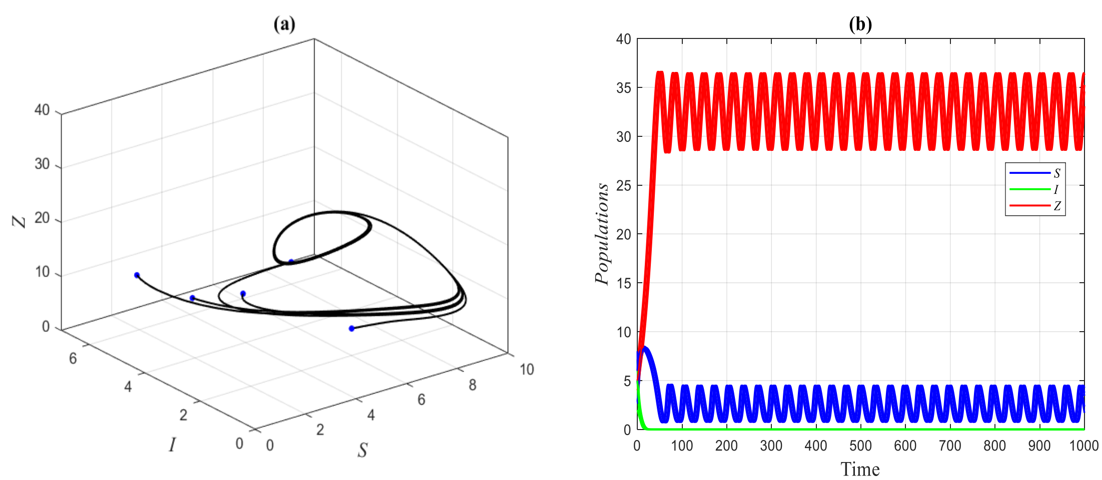

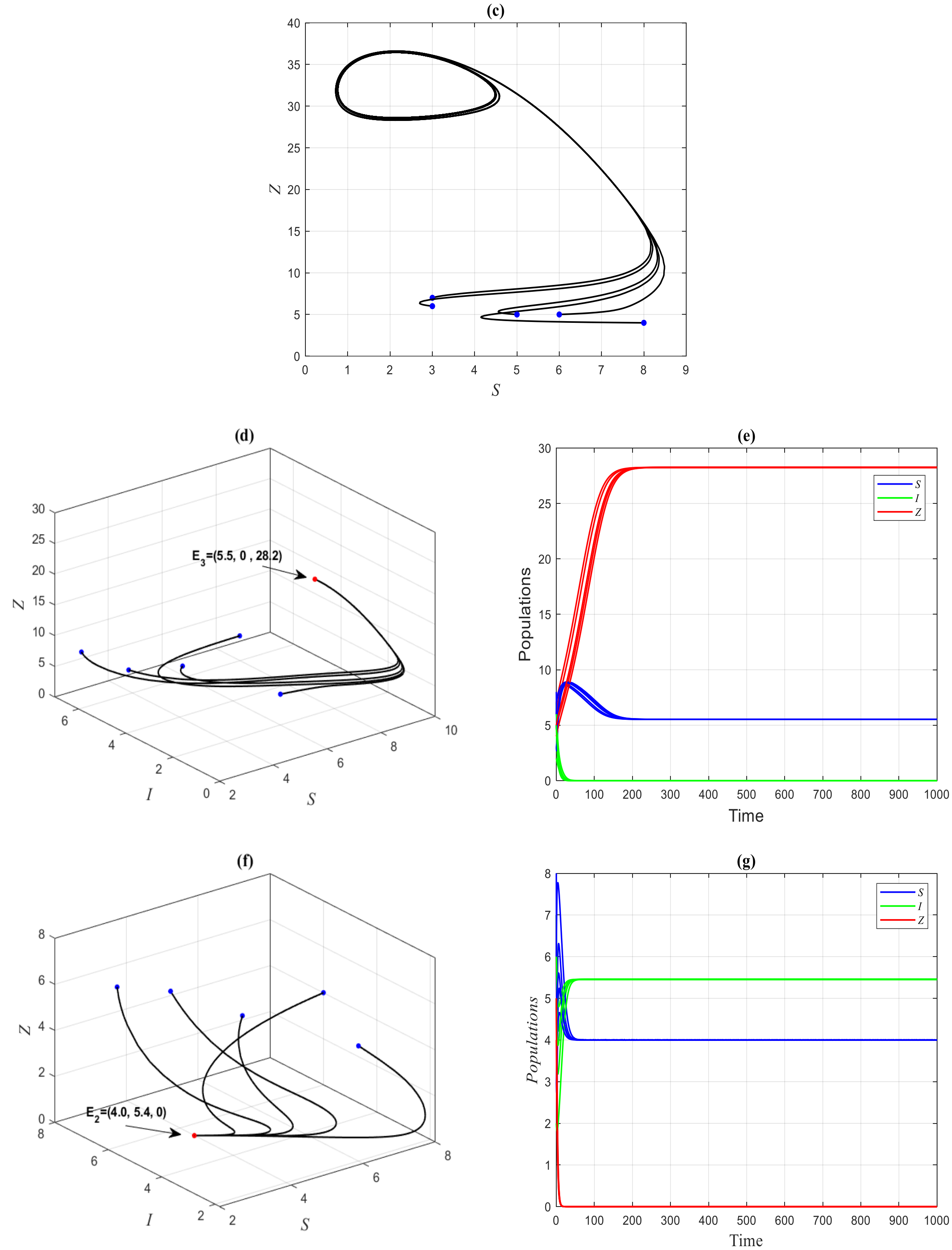

Figure 13. The trajectory of the system (1) utilizing the parameter values in table (1) with different values of θ_2. (a) Illustrates the phase portrait when $\theta_2 = 0.04$. (b) Shows the time series of (a). (c) Illustrates the projection on the $SZ-$plane. (d) Illustrates the phase portrait when $\theta_2 = 0.07$. (e) Shows the time series of (d). (f) Illustrates the phase portrait when $\theta_2 = 0.5$. (g) Shows the time series of (f).

10. CONCLUSION AND DISCUSSION

The effects of wind and disease are explored from a dynamics viewpoint in this paper utilizing a prey-predator model. The properties of the solution are demonstrated. The existence of equilibrium points and their stability are investigated. The persistence of system (1) are explained. The global stability of all possible equilibrium points is employed. The local bifurcation around the equilibrium points are investigated.

System (1) is solved numerically utilizing a set of parameter values as in table (1) and starting from various initial points to confirm the analytical results which obtained and understand the effect of changing the parameter values. It is spotted that the system has various types of dynamics. It is noticed that decreasing the intrinsic growth rate, the attack rate of the predator on the infected prey and conversion rate from infected prey below the specific value, lead to lose the persistence, and the trajectory goes to the PF-EP.

On the other side, decreasing the attack rate of the predator on the susceptible prey and conversion rate from susceptible prey below a specific value lead to loss of persistence, and the trajectory goes to the PF-EP. While increasing of them above a specific value lead to loss of persistence, and the trajectory goes to the IPF-EP. Furthermore, increasing them further above a specific value lead to loss of persistence, and the trajectory goes to a periodic oscillation in the $SZ-$ plane.

On the other hand, decreasing the carrying capacity below a specific value lead to loss of persistence, and the trajectory goes to the PF-EP. While decreasing further lead to loss of persistence, and the trajectory goes to the AEP. Moreover, increasing it above a specific value lead to loss of persistence, and the trajectory goes to IPF-EP. Whilst increasing it further lead to loss of persistence, and the trajectory goes to a periodic oscillation in the $SZ-$ plane.

Moreover, increasing (decreasing) the infection rate above (below) a specific value lead to loss of persistence, and the trajectory goes to the PF-EP. While decreasing it further lead to loss of persistence, and the trajectory goes to the AEP. However, decreasing the wind flow below a specific value lead to loss of persistence, and the trajectory goes to the IPF-EP. While increasing it further lead to loss of persistence, and the trajectory goes to the PF-EP.

Also, decreasing the hindrance rate in susceptible prey catching for the predator below a specific value lead to loss of persistence, and the trajectory goes to the IPF-EP.

Furthermore, increasing the hindrance rate in infected prey catching for the predator above a specific value lead to loss of persistence, and the trajectory goes to the PF-EP. On the other hand, increasing the mortality rate of predator above a specific value lead to loss of persistence, and the trajectory goes to the AEP. Finally, increasing the mortality rate of infected prey above a specific value lead to loss of persistence, and the trajectory goes to the PF-EP. Moreover, decreasing it below a specific value lead to loss of persistence, and the trajectory goes to the IPF-EP. While decreasing it further lead to loss of persistence, and the trajectory goes to a periodic oscillation in the $SZ-$ plane.

Therefore, the previous conclusions explained that system (1) is sensitive to varying the parameter values. In this paper, the future direction will be discussed as follows
For the suggested a prey-predator model which involving the wind flow and disease in prey, it's possible to develop it. Various types of functional responses which describing the process of predation. In addition to studying the impact of time delays on the ecosystem.

CONFLICT OF INTERESTS

The authors declare that there is no conflict of interests.

REFERENCES

[1] S. Hsu, T. Hwang, Y. Kuang, Global Analysis of the Michaelis-Menten-Type Ratio-Dependent Predator-Prey System, J. Math. Biol. 42 (2001), 489-506. https://doi.org/10.1007/s002850100079.

[2] R.K. Naji, A. Balasim, On the Dynamical Behavior of Three Species Food Web Model, Chaos, Solitons Fractals 34 (2007), 1636-1648. https://doi.org/10.1016/j.chaos.2006.04.064.

[3] X. Liu, Y. Lou, Global Dynamics of a Predator–prey Model, J. Math. Anal. Appl. 371 (2010), 323-340. https://doi.org/10.1016/j.jmaa.2010.05.037.

[4] R.K. Naji, R.K. Upadhyay, V. Rai, Dynamical Consequences of Predator Interference in a Tri-Trophic Model Food Chain, Nonlinear Anal.: Real World Appl. 11 (2010), 809-818. https://doi.org/10.1016/j.nonrwa.2009.01.026.

[5] E. González-Olivares, A. Rojas-Palma, Multiple Limit Cycles in a Gause Type Predator–prey Model with Holling Type III Functional Response and Allee Effect on Prey, Bull. Math. Biol. 73 (2010), 1378-1397. https://doi.org/10.1007/s11538-010-9577-5.

[6] X. Yu, F. Sun, Global Dynamics of a Predator-Prey Model Incorporating a Constant Prey Refuge, Electron. J. Differ. Equ. 2013 (2013), 1-8.

[7] J. Llibre, D. Xiao, Global Dynamics of a Lotka--Volterra Model with Two Predators Competing for One Prey, SIAM J. Appl. Math. 74 (2014), 434-453. https://doi.org/10.1137/130923907.

[8] C. Xu, S. Yuan, T. Zhang, Global Dynamics of a Predator–prey Model with Defense Mechanism for Prey, Appl. Math. Lett. 62 (2016), 42-48. https://doi.org/10.1016/j.aml.2016.06.013.

[9] N.H. Fakhry, R.K. Naji, The Dynamics of a Square Root Prey-Predator Model with Fear, Iraqi J. Sci. 61 (2020), 139-146. https://doi.org/10.24996/ijs.2020.61.1.15.

[10] A.J. Lotka, Elements of Physical Biology, Williams & Wilkins, 1925.

[11] V. Volterra, Variazioni e Fluttuazioni del Numero di Individui in Specie Animali Conviventi, Mem. Acad. Lincei. 2 (1926), 31-113.

[12] R.K. Naji, On the Dynamical Behavior of a Prey-Predator Model with the Effect of Periodic Forcing, Baghdad Sci J. 4 (2021), 147-157.

[13] F.H. Maghool, R.K. Naji, The Dynamics of a Tritrophic Leslie-Gower Food-Web System with the Effect of Fear, J. Appl. Math. 2021 (2021), 2112814. https://doi.org/10.1155/2021/2112814.

[14] H. Abdul Satar, R.K. Naji, Stability and Bifurcation of a Prey-Predator-Scavenger Model in the Existence of Toxicant and Harvesting, Int. J. Math. Math. Sci. 2019 (2019), 1573516. https://doi.org/10.1155/2019/1573516.

[15] D.K. Bahlool, The Dynamics of a Stage-Structure Prey-Predator Model with Hunting Cooperation and Anti-Predator Behavior, Commun Math Biol Neurosci. 2023 (2023), 59. https://doi.org/10.28919/cmbn/8003.

[16] H.A. Ibrahim, R.K. Naji, Chaos in Beddington–deangelis Food Chain Model with Fear, J. Phys.: Conf. Ser. 1591 (2020), 012082. https://doi.org/10.1088/1742-6596/1591/1/012082.

[17] , The Invasion, Persistence and Spread of Infectious Diseases Within Animal and Plant Communities, Philos. Trans. R. Soc. Lond. B, Biol. Sci. 314 (1986), 533-570. https://doi.org/10.1098/rstb.1986.0072.

[18] A.K.K. Pal, G.P.P. Samanta, Stability Analysis of an Eco-Epidemiological Model Incorporating a Prey Refuge, Nonlinear Anal.: Model. Control. 15 (2010), 473-491. https://doi.org/10.15388/na.15.4.14319.

[19] R.K. Naji, A.N. Mustafa, The Dynamics of an Eco‐epidemiological Model with Nonlinear Incidence Rate, J. Appl. Math. 2012 (2012), 852631. https://doi.org/10.1155/2012/852631.

[20] B. Sahoo, S. Poria, Diseased Prey Predator Model with General Holling Type Interactions, Appl. Math. Comput. 226 (2014), 83-100. https://doi.org/10.1016/j.amc.2013.10.013.

[21] H. Abdul Satar, H.A. Ibrahim, D.K. Bahlool, On the Dynamics of an Eco-Epidemiological System Incorporating a Vertically Transmitted Infectious Disease, Iraqi J. Sci. 62 (2021), 1642-1658. https://doi.org/10.24996/ijs.2021.62.5.27.

[22] S. Bera, A. Maiti, G. Samanta, A Prey-Predator Model with Infection in Both Prey and Predator, Filomat 29 (2015), 1753-1767. https://doi.org/10.2298/fil1508753b.

[23] A.S. Abdulghafour, R.K. Naji, A Study of a Diseased Prey-Predator Model with Refuge in Prey and Harvesting from Predator, J. Appl. Math. 2018 (2018), 2952791. https://doi.org/10.1155/2018/2952791.

[24] A. Hugo, E. Simanjilo, Analysis of an Eco-Epidemiological Model under Optimal Control Measures for Infected Prey, Appl. Appl. Math.: Int. J. 14 (2019), 117-138.

[25] W. Hussein, H. Abdul Satar, The the Dynamics of a Prey-Predator Model with Infectious Disease in Prey: Role of Media Coverage, Iraqi J. Sci. 62 (2021), 4930-4952. https://doi.org/10.24996/ijs.2021.62.12.31.

[26] A.F. Bezabih, G.K. Edessa, K.P. Rao, Ecoepidemiological Model and Analysis of Prey-Predator System, J. Appl. Math. 2021 (2021), 6679686. https://doi.org/10.1155/2021/6679686.

[27] A. Savadogo, B. Sangaré, H. Ouedraogo, A Mathematical Analysis of Prey-Predator Population Dynamics in the Presence of an Sis Infectious Disease, Res. Math. 9 (2022), 2020399. https://doi.org/10.1080/27658449.2021.2020399.

[28] H.A. Ibrahim, R.K. Naji, A Prey-Predator Model with Michael Mentence Type of Predator Harvesting and Infectious Disease in Prey, Iraqi J. Sci. 61 (2020), 1146-1163. https://doi.org/10.24996/ijs.2020.61.5.23.

[29] M.S. Rahman, S. Chakravarty, A Predator-Prey Model with Disease in Prey, Nonlinear Anal.: Model. Control. 18 (2013), 191-209. https://doi.org/10.15388/na.18.2.14022.

[30] S. Jana, T. Kar, Modeling and Analysis of a Prey–predator System with Disease in the Prey, Chaos, Solitons Fractals 47 (2013), 42-53. https://doi.org/10.1016/j.chaos.2012.12.002.

[31] H.A. Ibrahim, On the Dynamical Behavior of an Eco-Epidemiological Model, Int J Nonlinear Anal. Appl. 12 (2021), 1749-1767. https://doi.org/10.22075/ijnaa.2021.5314.

[32] M. Haque, E. Venturino, Increase of the Prey May Decrease the Healthy Predator Population in Presence of a Disease in Predator, HERMIS 7 (2006), 38–59.

[33] M. Haque, A Predator–prey Model with Disease in the Predator Species Only, Nonlinear Anal.: Real World Appl. 11 (2010), 2224-2236. https://doi.org/10.1016/j.nonrwa.2009.06.012.

[34] K.P. Das, A Mathematical Study of a Predator-Prey Dynamics with Disease in Predator, ISRN Appl. Math. 2011 (2011), 807486. https://doi.org/10.5402/2011/807486.

[35] M.V.R. Murthy, D.K. Bahlool, Modeling and Analysis of a Prey-Predator System with Disease in Predator, IOSR J. Math. 12 (2016), 21–40.

[36] Y. Hsieh, C. Hsiao, Predator-prey Model with Disease Infection in Both Populations, Math. Med. Biol. 25 (2008), 247-266. https://doi.org/10.1093/imammb/dqn017.

[37] K.P. Das, K. Kundu, J. Chattopadhyay, A Predator–prey Mathematical Model with Both the Populations Affected by Diseases, Ecol. Complex. 8 (2011), 68-80. https://doi.org/10.1016/j.ecocom.2010.04.001.

[38] K.P. Das, S.K. Sasmal, J. Chattopadhyay, Disease Control through Harvesting-Conclusion Drawn from a Mathematical Study of a Predator-Prey Model with Disease in Both the Population, Int. J. Biomath. Syst. Biol. 1 (2014), 1-29.

[39] S. Kant, V. Kumar, Stability Analysis of Predator–prey System with Migrating Prey and Disease Infection in Both Species, Appl. Math. Model. 42 (2017), 509-539. https://doi.org/10.1016/j.apm.2016.10.003.

[40] A.R.M. Jamil, R.K. Naji, Modeling and Analysis of the Influence of Fear on the Harvested Modified Leslie–Gower Model Involving Nonlinear Prey Refuge, Mathematics 10 (2022), 2857. https://doi.org/10.3390/math10162857.

[41] Z. Zhang, R.K. Upadhyay, J. Datta, Bifurcation analysis of a modified Leslie–Gower model with Holling type-IV functional response and nonlinear prey harvesting. Adv. Differ. Equ. 2018 (2018), 127. https://doi.org/10.1186/s13662-018-1581-3.

[42] S.M.A. Al-Momen, R.K. Naji, The Dynamics of Modified Leslie-Gower Predator-Prey Model Under the Influence of Nonlinear Harvesting and Fear Effect, Iraqi J. Sci. 63 (2022), 259-282. https://doi.org/10.24996/ijs.2022.63.1.27.

[43] R.K. Naji, Contribution of Hunting Cooperation and Antipredator Behavior to the Dynamics of the Harvested Prey-Predator System, Commun. Math. Biol. Neurosci. 2023 (2023), 99. https://doi.org/10.28919/cmbn/8164.

[44] W. Zhang, D. Jin, R. Yang, Hopf Bifurcation in a Predator–prey Model with Memory Effect in Predator and Anti-Predator Behaviour in Prey, Mathematics 11 (2023), 556. https://doi.org/10.3390/math11030556.

[45] W. Qin, Z. Dong, L. Huang, Impulsive Effects and Complexity Dynamics in the Anti-Predator Model with IPM Strategies, Mathematics 12 (2024), 1043. https://doi.org/10.3390/math12071043.

[46] Y. Enatsu, J. Roy, M. Banerjee, Hunting Cooperation in a Prey–predator Model with Maturation Delay, J. Biol. Dyn. 18 (2024), 2332279. https://doi.org/10.1080/17513758.2024.2332279.

[47] S.R. Jang, A.M. Yousef, Effects of Prey Refuge and Predator Cooperation on a Predator–prey System, J. Biol. Dyn. 17 (2023), 2242372. https://doi.org/10.1080/17513758.2023.2242372.

[48] Y. Du, B. Niu, J. Wei, Dynamics in a Predator–prey Model with Cooperative Hunting and Allee Effect, Mathematics 9 (2021), 3193. https://doi.org/10.3390/math9243193.

[49] M. Haque, S. Sarwardi, Dynamics of a Stage-Structured-Prey and Predator Model with Linear Harvesting of Mature Prey and Predator, Interdiscip. J. Discontinuity, Nonlinearity, Complex. 10 (2021), 61-75. https://doi.org/10.5890/dnc.2021.03.005.

[50] Y. Li, Z. Lv, X. Fan, Bifurcations of a Diffusive Predator-prey Model with Prey‐stage Structure and Prey‐taxis, Math. Methods Appl. Sci. 46 (2023), 18592-18604. https://doi.org/10.1002/mma.9581.

[51] H.A. Ibrahim, R.K. Naji, The Impact of Fear on a Harvested Prey–predator System with Disease in a Prey, Mathematics 11 (2023), 2909. https://doi.org/10.3390/math11132909.

[52] J.M. Tylianakis, R.K. Didham, J. Bascompte, D.A. Wardle, Global Change and Species Interactions in Terrestrial Ecosystems, Ecol. Lett. 11 (2008), 1351-1363. https://doi.org/10.1111/j.1461-0248.2008.01250.x.

[53] D. Barman, V. Kumar, J. Roy, S. Alam, Modeling Wind Effect and Herd Behavior in a Predator–prey System with Spatiotemporal Dynamics, Eur. Phys. J. Plus 137 (2022), 950. https://doi.org/10.1140/epjp/s13360-022-03133-4.

[54] E.M. Takyi, K. Cooper, A. Dreher, C. McCrorey, Dynamics of a Predator–prey System with Wind Effect and Prey Refuge, J. Appl. Nonlinear Dyn. 12 (2023), 427-440. https://doi.org/10.5890/jand.2023.09.001.

[55] P. Panja, Impacts of Wind and Anti-Predator Behaviour on Predator-Prey Dynamics: a Modelling Study, Int. J. Comput. Sci. Math. 15 (2022), 396-407. https://doi.org/10.1504/ijcsm.2022.125906.

[56] D. Barman, J. Roy, S. Alam, Impact of Wind in the Dynamics of Prey–predator Interactions, Math. Comput. Simul. 191 (2022), 49-81. https://doi.org/10.1016/j.matcom.2021.07.022.

[57] L. Perko, Differential Equations and Dynamical Systems. Springer, 2001.